

Variability of the quasi-2-day wave observed in the MLT region during the PSMOS campaign of June–August 1999

D. Pancheva^{a,*}, N.J. Mitchell^a, A.H. Manson^b, C.E. Meek^b, Ch. Jacobi^c,
Yu. Portnyagin^d, E. Merzlyakov^d, W.K. Hocking^e, J. MacDougall^e, W. Singer^f,
K. Igarashi^g, R.R. Clark^h, D.M. Rigginⁱ, S.J. Franke^j, D. Kürschner^k,
A.N. Fahrutdinova^l, A.M. Stepanov^l, B.L. Kashcheyev^m, A.N. Oleynikov^m,
H.G. Mullerⁿ

^aDepartment of Electronic and Electrical Engineering, University of Bath, Bath BA2 7AY, UK

^bInstitute of Space and Atmospheric Studies, University of Saskatchewan, Saskatoon, Canada

^cInstitute for Meteorology, University of Leipzig, Leipzig, Germany

^dInstitute for Experimental Meteorology, Obninsk, Russia

^eUniversity of Western Ontario, London, Canada

^fLeibniz Institute of Atmospheric Physics, Kühlungsborn, Germany

^gCommunications Research Laboratory, Koganei, Tokyo, Japan

^hUniversity of New Hampshire, Durham, USA

ⁱColorado Research Associates, Boulder, Colorado, USA

^jUniversity of Illinois, Urbana, USA

^kInstitute for Geophysics and Geology, University of Leipzig, Collm Observatory, Germany

^lKazan State University, Kazan, Russia

^mKharkov State Technical University of Radioelectronics, Kharkov, Ukraine

ⁿUniversity of Cranfield, RMCS, Shrivenham, Swindon, UK

Received 10 February 2003; accepted 20 January 2004

Abstract

A network of 15 northern hemisphere radars has been used to measure horizontal winds in the mesosphere and lower thermosphere during the PSMOS campaign of Summer 1999. The radars are sited at latitudes ranging from 21°N to 75°N and longitudes from 142°E to 157°W. The data were examined to investigate the Northern Hemisphere structure of the quasi-2-day planetary wave during the interval June–August. The amplitude of the 2-day wave was found to exhibit great day-to-day variability. In particular, significant periodic fluctuations in amplitude occurred with periods of 8–10 and 14–17 days. These modulations were strongest in July and largely absent in June and August. In July, the wave activity can be resolved into three westward-propagating waves with zonal wave numbers of 2, 3 and 4. The periods associated with these wave numbers were 53–56, 48–50 and 42–43 h, respectively. The simultaneous presence of at least two spectral components with periods close to each other may serve to explain the observed amplitude modulations as a result of a beating between different spectral components. An earlier analysis of the planetary-wave field during this interval has revealed a westward propagating ~16-day wave with zonal wave number 1 (Journal of Atmospheric and Solar-Terrestrial Physics 64 (2002b) 1865–1896). A non-linear interaction between this ~16-day planetary wave and the (3,0) Rossby-gravity mode (the 2-day-wave) provides a possible mechanism to generate the above ~42 h/wavenumber 4 wave and the ~55 h/wavenumber 2 waves as sum and difference secondary waves. A bispectral analysis was used to further investigate non-linear interactions between members of the planetary-wave field and suggested a number of interactions occur within

* Corresponding author. Tel.: +44-1225-826310; fax: +44-1225-826305.

E-mail address: eesdvp@bath.ac.uk (D. Pancheva).

the planetary-wave field, but that some of the interactions also involve the non-migrating diurnal tide with zonal wavenumber 6.
© 2004 Elsevier Ltd. All rights reserved.

Keywords: MLT dynamics; Waves and tides; Non-linear interactions

1. Introduction

The quasi-2-day planetary wave can be a dominant feature of the motion field of the mesosphere/lower thermosphere (MLT) region. The wave is a large-amplitude global-scale oscillation and has been observed by various ground-based and satellite techniques over the last three decades. The general characteristics of the wave are now reasonably well known. At middle and high-middle latitudes the wave has been observed at all levels in the mesosphere and is known to have two distinct activity maxima—one during summer after the summer solstice and one (generally weaker) during the winter months (e.g., Manson et al., 2004). In the northern hemisphere, the wave amplitudes maximize near the mesopause in July–August and there is a corresponding southern hemisphere maximum in January–February. Recent studies at polar latitudes have revealed that wave activity in the winter polar mesosphere (November–February) is stronger than in summer months (May–August) (Nozawa et al., 2003). At tropical and equatorial latitudes, wave activity is strong in both summer and winter seasons, and can reach particularly large amplitudes in January–February (e.g., Harris and Vincent, 1993; Palo and Avery, 1995; Gurubaran et al., 2001). A great range of vertical wavelengths have been measured, with values reported ranging from as little as 20 km to more than 150 km.

At all latitudes, the wave is observed to reach maximum amplitudes at heights in the range of 80–100 km. The peak amplitudes can reach very large values, sometimes in excess of 40–60 m/s, making the 2-day wave the largest amplitude feature of the MLT region. At mid-latitudes, the meridional component of the amplitude is usually larger than the zonal by a factor of ~ 1.5 (e.g., Clark et al., 1994). This polarization is particularly apparent in the Southern Hemisphere, although in the Northern Hemisphere the amplitude ratio may sometimes be closer to unity (e.g., Jacobi et al., 1997, 1998). At polar latitudes the ratio of the meridional to zonal amplitudes is found to be less, and in the range ~ 1.1 – 1.2 (Nozawa et al., 2003).

Hemispheric asymmetries are also apparent in the behaviour of the wave. The amplitude of the wave is generally larger in the Southern Hemisphere, and mean amplitudes can be up to a factor of 2 greater than those of the Northern Hemisphere. In the Southern Hemisphere the wave period is often found to be close to exactly 48 h, while in the Northern Hemisphere measurements it varies between 42 and 56 h.

The quasi-2-day wave in the middle atmosphere has been extensively studied by ground-based radar systems (e.g., Muller, 1972; Salby and Roper, 1980;

Craig et al., 1980; Plumb et al., 1987; Tsuda et al., 1988; Raghava Reddi et al., 1988; Harris and Vincent, 1993; Palo and Avery, 1995; Jacobi et al., 1997; Thayaparan et al., 1997a; Gurubaran et al., 2001), by rocket-sonde measurements of winds in the upper stratosphere (Coy, 1979) and by satellites (e.g., Rodgers and Prata, 1981; Burks and Leovy, 1986; Wu et al., 1993; Ward et al., 1996; Lieberman, 1999).

A number of studies have used longitudinally spaced networks of ground-based radars and been able to determine the zonal structure of the wave. In the Southern Hemisphere, the dominant structure of the wave is a westward propagating pattern of zonal wavenumber 3. In the Northern Hemisphere, the observed zonal wavenumbers reported range between 2 and 5, although the wavenumber 3 structure is still the most significant (e.g., Muller and Nelson, 1978; Meek et al., 1996; Thayaparan et al., 1997b). Satellite analyses have also indicated a westward propagating structure with zonal wavenumbers between 2 and 4 (e.g., Lieberman, 1999, 2002).

Two distinct mechanisms have been proposed as possible causes of the excitation of the 2-day wave in the middle atmosphere. The first is based on normal mode theory and interprets the wave as a manifestation of the (3,0) Rossby-gravity mode (Salby, 1981a). In an ideal atmosphere, the (3,0) Rossby-mode is a natural, unforced, resonant solution with a period of 2.1 days, zonal wavenumber 3 and westward propagation. Salby (1981a, b) used a mechanistic model based on the linearized perturbation equations to show that the (3,0) Rossby-mode will produce a significant response near the time of the solstice. These simulations were based on analytical background wind and temperature fields. More recently, Hagan et al. (1993) have extended the results of Salby (1981b) by using the two-dimensional Global Scale Wave Model (GSWM) under January solstice conditions with three different global mean wind fields. They found that the stratospheric and mesospheric zonal mean winds strongly affect the features of the 2-day wave observed in the MLT region.

In contrast, Plumb (1983) and Pfister (1985) proposed an alternative explanation based on instability theory for the excitation of the 2-day wave. Using a one-dimensional model, Plumb (1983) showed that a 2-day wave with a zonal wavenumber 3 can develop as an unstable perturbation of the summertime mesospheric easterly jet. On the basis of two-dimensional stability analysis, Pfister (1985) obtained peaks in the unstable wave growth spectrum at zonal wavenumbers 2–4 with periods 1.4–3 days for a variety of basic state flows. The geopotential response of the Pfister model is generally trapped between

40° and 60°, although observation reveals a more global structure.

Both modelling and observational studies have produced evidence supporting the normal mode and instability hypotheses. The close matching between the parameters of the unstable and free modes led Randel (1994) to suggest that the observed 2-day wave is a mixture of a global, near-resonant oscillation excited by baroclinic instability.

Norton and Thuburn (1996) proposed that the quasi-2-day wave is connected to both these mechanisms, and that a baroclinic instability provides an initial forcing that is subsequently followed by a normal mode response giving rise to the large-scale global responses observed.

Salby and Callaghan (2001) explored the relationship between the two suggested excitation mechanisms described above. In a model-based study, they suggested that under solstice conditions the 2-day Rossby-gravity wave receives additional, auxiliary forcing from the instability of the summertime mesospheric jet. This forcing alters the mode's growth rate and is sensitive to the structure of the mean zonal flow, but has little effect on the 2-day wave's period and structure.

The 2-day wave itself is known to display considerable variability on a range of timescales. In addition to the well-known inter-annual and short-term changes in wave amplitude (e.g., Harris and Vincent, 1993; Clark et al., 1994), considerable day-to-day variability of the period has also been reported (e.g., Tsuda et al., 1988; Williams and Avery, 1992). Jacobi et al. (1998) analysed 14 years of summertime MLT region wind data and showed that the amplitude of the 2-day wave is modulated by other lower frequency, planetary waves, and in particular the well-known 10- and 16-day waves. Subsequently, Pancheva et al. (2000) applied a wavelet and bispectral analysis to meteor-radar MLT data to suggest that a variety of interactions occur between different members of the ensemble of planetary waves at MLT heights. The largest amplitude planetary waves appear to be associated with the strongest interactions, particularly the 2-day wave in summer, which interacts with the 10- and 16-day waves. This coupling between the 2-day wave and the longer period planetary waves is responsible not only for a significant contribution to the observed variability of the 2-day wave amplitudes, but also generates a number of "secondary" waves with periods near 2 days.

The PSMOS programme carried out a 3-month long dedicated global campaign, *Global Scale Tidal Variability*, designed to measure the winds, waves and tides of the summertime Northern Hemisphere MLT region in 1999. The main objective of the campaign was to study the global structure and variability of the 12- and 24-h tides. Because the 2-day wave appears to contribute significantly to the variability of the 12-h tide, the campaign was chosen to take place during the time when the 2-day wave maximizes in the Northern Hemisphere, and so spanned the interval June 1–August 31, 1999. The great majority of ground-based instruments used

in this campaign were meteor and MF radars. The results of this campaign with respect to the global-scale tidal structures and variability have been reported elsewhere (Pancheva et al., 2002a, b). The data set from this campaign is, of course, well suited to study the 2-day wave itself. The behaviour of the 2-day wave during the northern summertime PSMOS campaign of 1999 is addressed in this paper.

2. Observations and analysis of the radar data

The data analysed and presented here were recorded by 15 ground-based systems, mostly medium frequency (MF) and meteor wind (MW) radars, although some data were also provided by low frequency D1 ionospheric drift measurements. Table 1 lists the locations of the various instruments used and presents some notes on the data obtained from them. A detailed description of the different types of instruments participating in the Summer 1999 campaign has been presented by Pancheva et al. (2002a). Two of the MW radars used operated without routine height finding and so the measurements are assumed to yield winds representative of range 90–95 km. Three other radars provided data only for one level (either 94 or 95 km). The remaining 10 radars were able to make measurements from at least at two heights in the range 89–96 km (see Table 1), and so provided data with some information on the vertical structure of the 2-day wave.

The analysis proceeded by first calculating time series of hourly mean zonal and meridional winds for each site. The 2-day wave itself was studied by using two methods: a complex demodulation method and a least-squares best-fit (with changing 2-day wave period). The complex demodulation method is usually used for effective investigation of one frequency range at a time (Bloomfield, 1976). We applied this method here because some observations, especially from the Northern Hemisphere, showed that the period of the quasi-2-day wave varies from between 40 and 60 h. This technique allows the amplitude and phase of an oscillation to be described as a function of time. The basic concepts of this analysis and its application to the case of the 2-day wave have been described in detail elsewhere (Harris and Vincent, 1993; Thayaparan et al., 1997a).

To further reveal the winds, tides and 2-day wave we also used a simple linear least-squares fitting algorithm. The time series of winds were fitted with a superposition of a mean wind, 2-day wave and 24-, 12- and 8-h tides. The wave period of the 2-day wave was varied systematically from 40 to 60 h in steps of 0.5 h. This was carried out in order to provide maximum sensitivity to amplitude variations. The data points were weighted in the fitting process according to the number of individual measurements comprising each hourly mean (when such information was available). Otherwise, all data points were equally weighted in the fitting process. For those instruments with height resolution, each height was treated separately.

Table 1

The locations of the various instruments used during PSMOS campaign and some notes on the data obtained from them

Station	Instrument	Location	Height (km)	Period of measurements
Resolute Bay, Canada	Meteor radar	75°N, 95°W	94	01 June–31 July
Andenes, Norway	MF radar	69°N, 19°E	90–94	01 June–31 August
Kazan, Russia	Meteor radar	56°N, 49°E	90–94	25 June–31 August
Juliusruh, Germany	MF radar	55°N, 13°E	89–95	01 June–31 August
Obninsk, Russia	Meteor radar	55°N, 37°E	No height resolution	01 July–31 August
Saskatoon, Canada	MF radar	52°N, 107°W	91–94	01 June–31 August
Collm, Germany	LF D1 method	52°N, 15°E	95	01 June–31 August
Castle Eaton, UK	Meteor radar	52°N, 2°W	No height resolution	01 June–31 August
Kharkov, Ukraine	Meteor radar ^a	50°N, 36°E	90–96	01 July–31 August
Wakkanai, Japan	MF radar	45°N, 142°E	90–96	01 June–20 August
London Ontario, Canada	MF radar	43°N, 81°W	91–94	01 June–19 August
Durham, USA	Meteor radar	43°N, 71°W	95	01 June–31 August
Urbana, USA	MF radar	40°N, 88°W	90–96	07 June–31 August
Yamagawa, Japan	MF radar	31°N, 131°E	90–96	01 June–29 July
Hawaii	MF radar	21°N, 157°W	90–94	01 June–26 August

^aOnly zonal wind component.

The tidal and 2-day wave characteristics were determined by applying these analysis techniques to data segments of 4-day duration. The 4-day segment was transferred through the time sequences in steps of 1 h and the analysis repeated, yielding hourly spaced values for the mean winds, the quasi-2-day wave and 24-, 12- and 8-h tidal amplitudes and phases. To estimate the confidence levels, we assumed that the residual fitting error is described by a Gaussian-white noise. The Student's *t*-test was then used to estimate the confidence levels.

A key aim of this paper is to study the global-scale variability of the quasi-2-day wave observed during the PSMOS campaign. It is well known that this wave is highly variable, with significant amplitude and phase changes occurring over relatively short timescales. The wavelet transform was used here to investigate this changing nature of the 2-day wave. The wavelet approach is becoming a favoured tool for analysing time series in which the assumption of stationarity does not hold. Decomposing the time series into time–frequency space, the wavelet transform is able to determine both the constituent frequencies and how those frequencies vary in time, producing a two-dimensional time–frequency image (e.g., Torrence and Compo, 1998).

The analysis presented here used the continuous Morlet wavelet, which consists of a plane wave modulated by a Gaussian envelope. The Morlet wavelet was selected because of its simplicity and resemblance to the modulated planetary-wave “packets”, which are frequently observed in the ionosphere and MLT region variability (Pancheva and Mukhtarov, 2000). However, it should be kept in mind that the choice of the wavelet type may itself impose biases in the analysis of the simultaneously occurring 2-day wave bursts with close periods. The localization characteristics in

time and frequency space of the Morlet wavelet used in this study (the wavelet frequency is 6) are as follows: the time localization, or the so-called “cone of influence”, is defined as a time interval which contributes to the wavelet coefficient at a given instant t_0 . In our case the influence cone is: $t \in [t_0 - \sqrt{2}a, t_0 + \sqrt{2}a]$ where a is the wavelet scale and $1.03a = T$, where T is the Fourier period. Likewise, the localization characteristics of the wavelet in frequency space gives local information about the studied function in frequency range: $\omega \in [\omega_0/a - 1/a\sqrt{2}, \omega_0/a + 1/a\sqrt{2}]$. The frequency resolution can be increased by using wavelet with higher than 6 intrinsic frequency, though at the expense of decreased time resolution.

Additional spectral information was gained by applying the high-resolution correlogram analysis (Kopecky and Kuklin, 1971). A description of the main advantage of this method to other techniques can be found in Apostolov et al. (1995). Here we note that this technique can give results superior to FFT method (for example), because it weights the data on a “per point” basis instead of on a “per time interval” basis.

A refinement of the wavelet analysis was used to investigate any periodicities simultaneously present in two or more time series. In this particular case, we apply a cross-wavelet analysis, where the cross-wavelet power serves as an indication for the strength of the oscillations co-existing in both time series, and the argument describes the phase difference between them.

The bispectral analysis was also applied to the time series of hourly data, in order to investigate the non-linear effects in the neutral MLT winds. The conventional “Fourier type” methods for bispectrum estimation can serve as reliable quantifiers of phase coupling, and therefore these

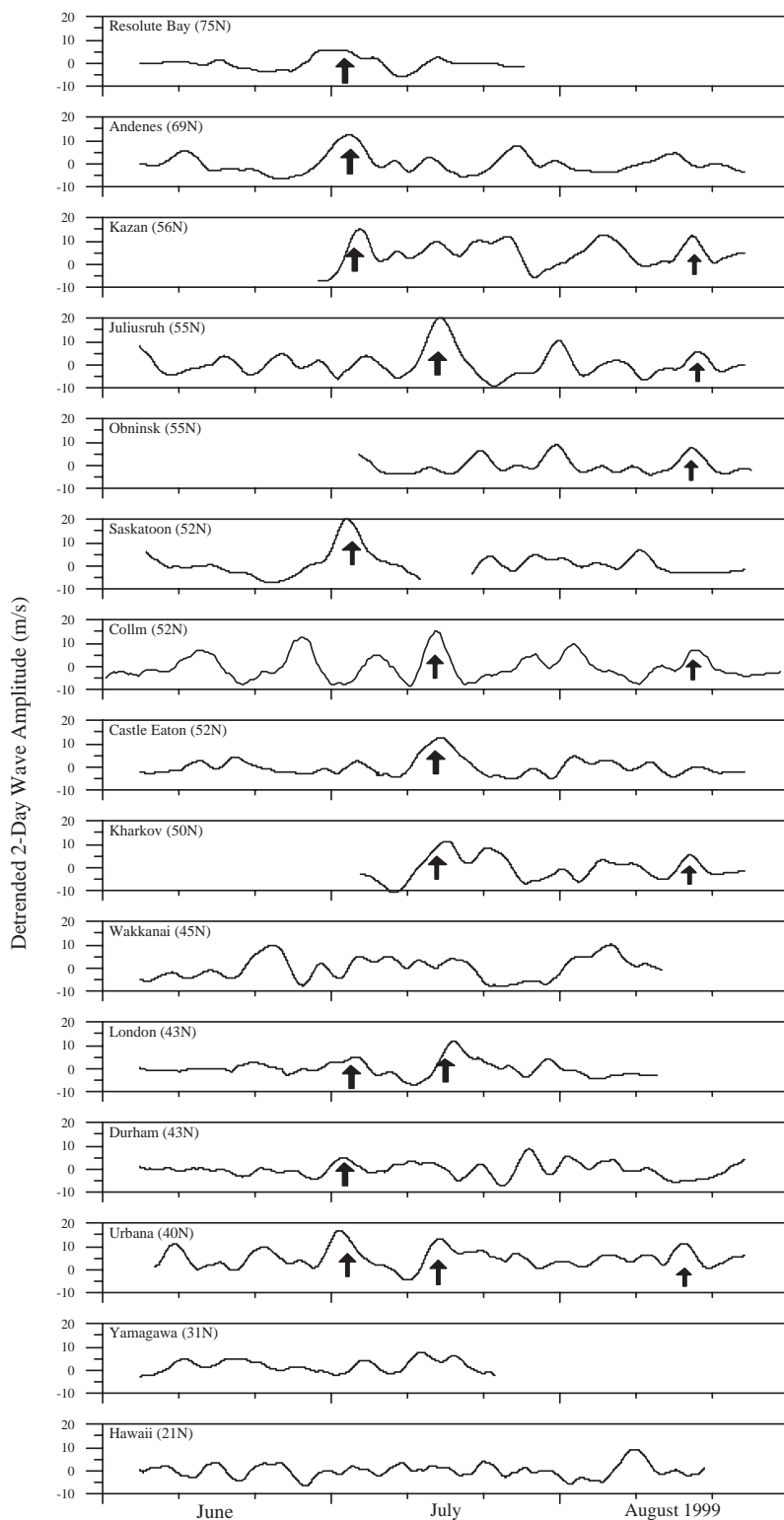


Fig. 1. Detrended and smoothed (by 3-day running mean) hourly values of the amplitudes of the quasi-2-day wave (obtained by complex demodulation) in the zonal wind for all stations in the Northern Hemisphere arranged according to their latitudes, starting from the most northern station Resolute Bay (75°N) and finishing with most southern one Hawaii (21°N). Arrows mark the amplifications of the 2-day wave activity evident at almost all sites.

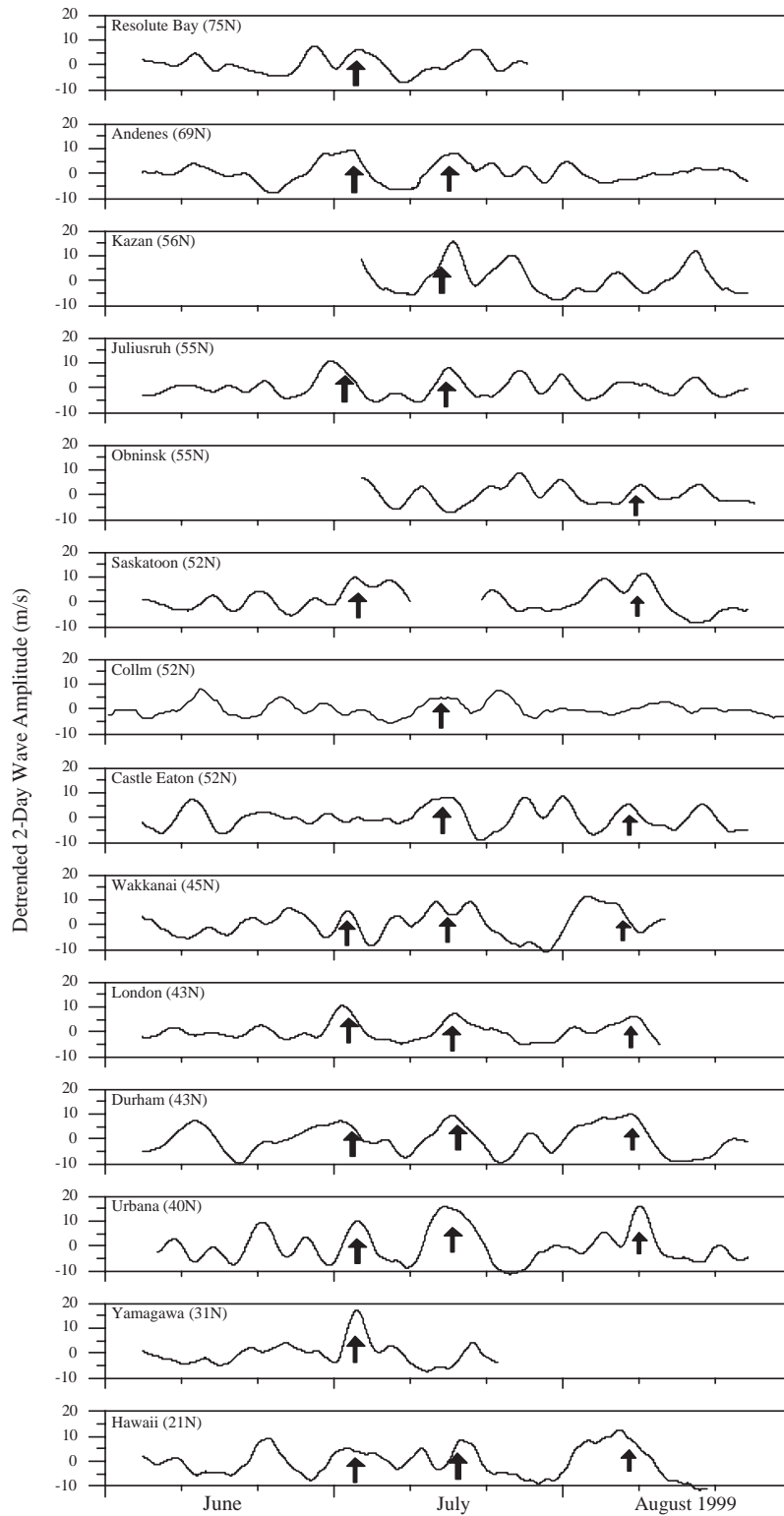


Fig. 2. The same as Fig. 1, but for the meridional wind.

techniques were used in investigating the non-linear interactions between waves in the atmosphere (Clark and Bergin, 1997; Beard et al., 1999; Pancheva, 2000). In the present work, the magnitude-squared bispectrum is calculated from the hourly values of zonal and meridional winds. The computational procedure is described in detail by Pancheva (2000).

A weakness of the wavelet transform and bispectral technique used here is that both require regularly spaced data points in the time series in consideration, i.e., there should be no gaps in the data. According to the length of data gap different filling procedures were applied. They are described in detail by Pancheva et al. (2002b).

3. Results

We will now consider the general vertical and latitudinal behaviour of the 2-day wave amplitudes observed during the summertime campaign. To find the amplitudes, a complex demodulation was applied to evaluate the temporal variation of the amplitude of the quasi-2-day wave (Bloomfield, 1976). A band-pass filter was used to reveal those oscillations with periods between 40 and 60 h for the 48-h demodulation period. We also applied the least-squares best-fit described above with periods varied between 40 and 60 h. In the fitting procedure we accepted those amplitudes of the quasi-2-day wave for which according to the Student's t -test the confidence level is equal or higher than 95%. The comparison showed that the wave amplitudes obtained by both methods are very similar. All analyses in this study were performed using both methods, but mainly the complex demodulation method will be shown in the final figures.

As mentioned above, some 10 of the MLT radars available provided data at two altitude levels, around 90 and 95 km. We used this information to investigate the vertical structure of the 2-day wave between these different heights. The comparison (not shown here) indicates that the behaviour of the 2-day wave amplitudes at both levels is very similar, with a slight tendency for the amplitudes to decrease with height. Because of this, we will hereafter only consider data from the lower height level. Note that some of the radars used in the study can in fact provide data over a much greater range of heights, but that the data used for the PSMOS experiment only used those data from 90 to 95 km.

The radars participating in this campaign covered a large range of geographical latitude and longitude (between 21°N and 75°N and between 142°E and 157°W). Table 1 lists the locations of the various instruments. Fig. 1 presents the detrended (a parabolic trend is present usually in the time series of the 2-day wave amplitudes) and smoothed (by 3-day running mean) amplitudes of the 2-day wave in the zonal wind observed at all stations arranged according to their latitude. The same analysis for the meridional wind is shown in Fig. 2. The time series reveal “bursts” of activity over most

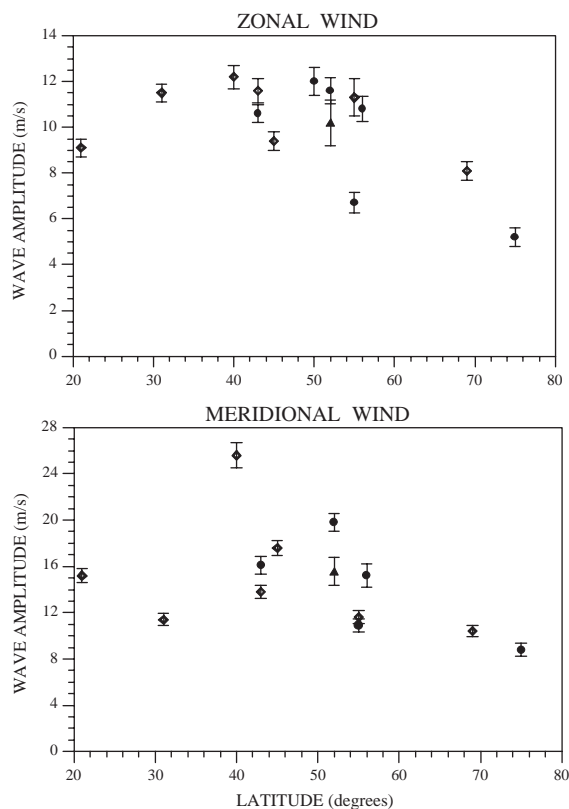


Fig. 3. Latitudinal variability of the average amplitudes of the 2-day wave observed during the interval 10–25 July, 1999, when the 2-day wave activity was strong. The upper panel shows the 2-day wave amplitudes in the zonal wind and the bottom panel—in the meridional wind. The results from different instruments are marked by different symbols: MF radar with empty diamond, MW radar with full dot and D1 LF drift measurements with triangle.

sites, marked by arrows in the figures. The main features of these figures can be summarized as follows:

- (i) The global character of the 2-day wave activity in the Northern Hemisphere is clearly evident. The strongest bursts of activity in the zonal wind component are observed at the end of June and July with a weaker moderate burst occurring in the second half of August. The strongest activity in the meridional component is observed also in July and there is also a long lasting burst in August.
- (ii) The 2-day wave activity in Summer 1999 is not exceptionally strong in either component and fits well into the long-term variation of 2-day wave amplitude (e.g., Jacobi, 1998).
- (iii) The day-to-day variability of the wave amplitude is considerable and quasi-periodic amplitude modulations with periods of ~ 9 – 10 and 14 – 15 days can be seen even from a casual inspection of the figures.

Figs. 1 and 2 also demonstrate the latitudinal variability of the wave amplitudes. The largest amplitudes for the zonal component occur at middle and high-middle latitudes (e.g., Kharkov, Castle Eaton and Collm). The largest amplitudes in the meridional component are seen at middle latitudes (e.g., Urbana, Wakkanai). A more detailed investigation of the latitudinal variability of the 2-day wave for the strong burst observed between 10 and 25 July is presented in Fig. 3 (upper panel for the zonal component, bottom panel for the meridional). Measurements made by the various techniques are indicated (MF radar with empty diamond, MW radar with full dot and D1 LF drift measurements with triangle). As can be seen from the figure, the latitudinal structure of the wave during this burst agrees well with the general pattern evident in Figs. 1 and 2. The 16-day averaged amplitudes for the zonal component observed in middle and high-middle latitudes reach 12 m/s, while those for the meridional component reach 18–20 m/s (only at Urbana do the amplitudes reach 26 m/s).

In the following sections we will consider the variability of the 2-day wave amplitude in detail and will consider possible causes of this variability.

3.1. 2-day wave activity in the zonal wind

Fig. 4 presents the wavelet transform of the amplitudes of the quasi-2-day wave obtained by a complex demodulation method (only Hawaii is missing because its amplitudes are very small comparing with the other sites, except a burst in the middle of August; see Fig. 1). The main features evident from the figure can be summarized as follows:

- (i) The modulation of the 2-day wave amplitudes takes place at almost all stations at the end of June/July, where the strongest bursts were observed (the moderate bursts in August do not show amplitude modulation for most of the stations);
- (ii) The modulations sometimes have two periods clustering around 9–10 and 14–17 days, although not all the stations observed the former (9–10-day) period modulation. At some stations the modulations with both periods can be seen (Obninsk and Durham, for example).

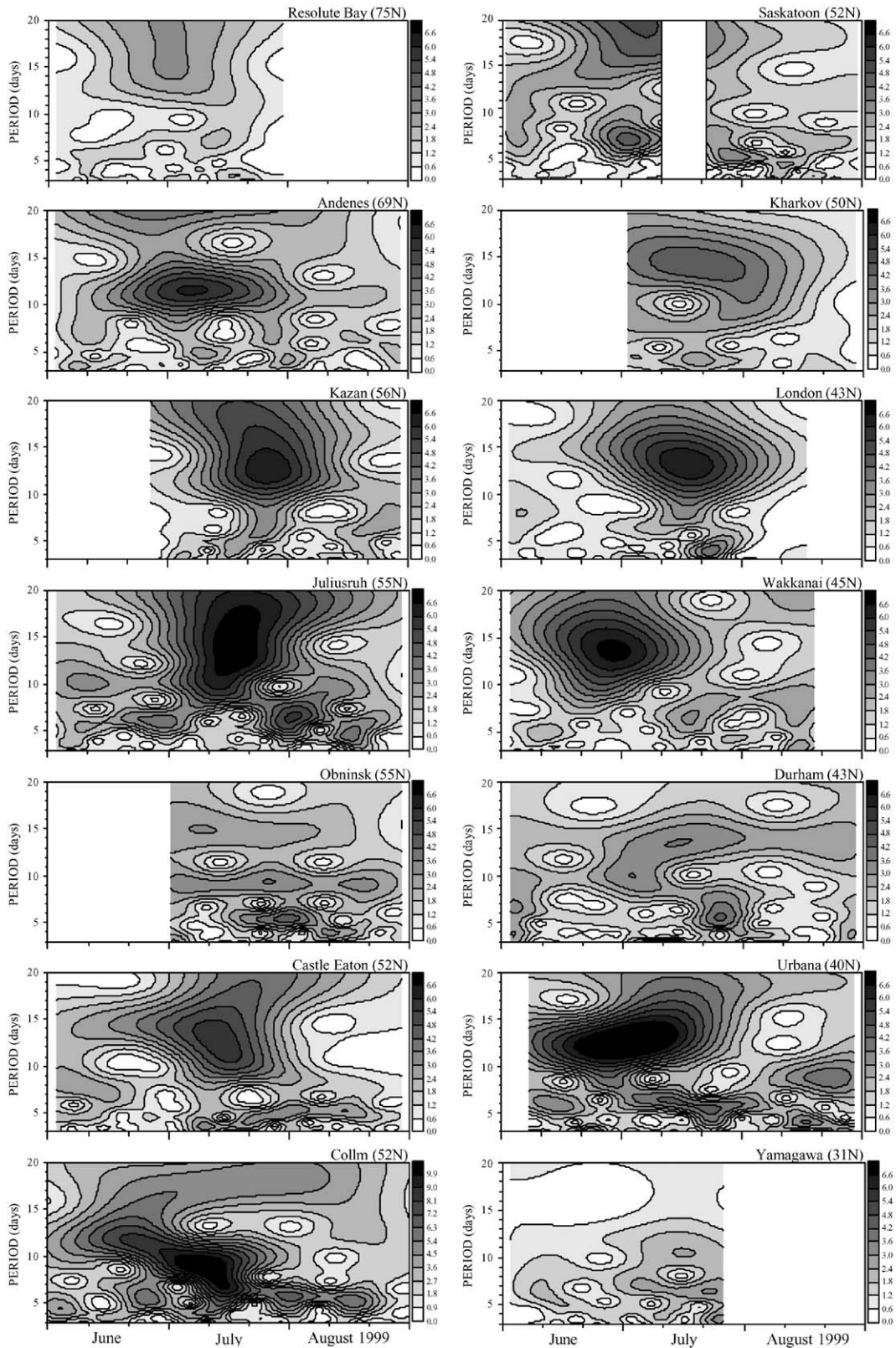
These observations raise the question as to what causes these global-scale amplitude modulations of the 2-day wave in the zonal wind observed at the end of June/July, and why for all sites the prevailing periods of these modulations are 9–10 and 14–17 days? A possible reason for the observed amplitude modulation is the simultaneous presence of more

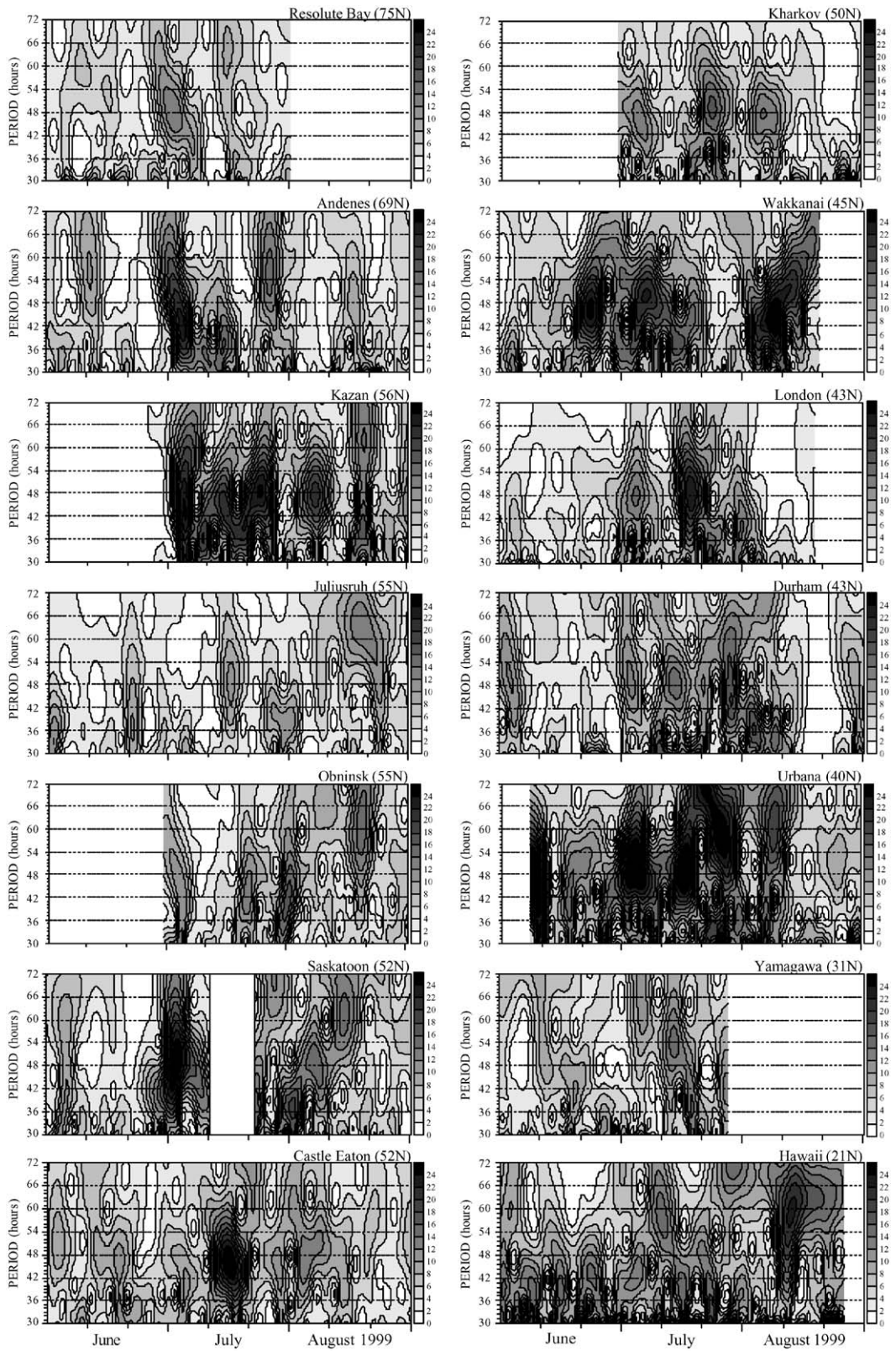
than one spectral component with a period near 2 days in the MLT region. Beating between spectral components with close periods would then produce amplitude modulations such as those evident in Fig. 4. Such closely spaced spectral components have been hypothesized to arise as a result of non-linear coupling between various tides and planetary waves in the MLT region (e.g., Pancheva et al., 2002b). Because we observe the amplitude modulation at the end of June/July and it is almost absent in August, this may indicate that in August the 2-day wave activity consists of only one spectral component.

To study in detail the 2-day wave bursts we performed the wavelet transform on the hourly zonal wind data in the period range between 30 and 72 h and the result for all sites is shown in Fig. 5 (the stations again are arranged according to their latitudes, starting from the most northern station Resolute Bay and finishing with Hawaii, the most southern one). For most of the sites the main 2-day wave activity is situated between June 25–August 10. After August 10, only a burst with period ~ 60 h can be easily distinguished. The 2-day wave bursts in the interval between June 25 and August 10 only the first burst, centred around June 30 for sites in middle and high latitudes, has period around 48 h, while for the remaining part of this interval we cannot determine some predominant spectral periods evident in most of the sites. This could be related to the wavelet-type spectra that may impose biases (related to the frequency resolution of the wavelet used) in the analysis of the wave bursts composed of two or more spectral components with close periods. To avoid this shortcoming of the Morlet wavelet analysis we return to the classical Fourier transform, assuming that the data are stationary enough to allow a spectrum calculation.

Fig. 6 (upper plot) shows the amplitude spectra derived from the hourly mean zonal winds measured between June 25 and August 10, for all sites that have at least one full month of continuous measurements. Three main peaks, marked by big arrows are clearly evident. They are centred at 42–43, 48–49 and 52–53 h. In each case the 95% confidence level is indicated. The spectra were calculated after removal of the linear or parabolic trend. We have to mention that there are sites where only two peaks are well above 95% confidence level (for example, the peak with period 48–49 h in Kharkov is weaker than the other two). To determine the zonal structure of these spectral components a least-squares best-fit procedure was applied to the time interval. The results are shown in Fig. 6 as well (lower plots). The left panel shows the longitudinal dependence of the derived phases of the oscillation with an average period of 42.5 h for the various sites. The slope of the fitted line obtained by a weighted least-squares best-fit line is

Fig. 4. The wavelet transform of the hourly values of the amplitudes of 2-day wave in the zonal wind (obtained by complex demodulation) at all sites shown in Fig. 1 (except Hawaii, see text). The results are arranged in the same way as in the Fig. 1 starting from Resolute Bay (the upper left figure) and ending at Yamagawa (the lowest right figure).





-3.88 ± 0.19 . This indicates a westward-propagating wave with zonal wavenumber 4. The slope of the second spectral component (middle panel) with an average period of 48.5 h is -3.06 ± 0.09 , this again indicates a westward-propagating wave however, the zonal wavenumber is 3. The slope of the third spectral component (right panel) with a mean period of 52.5 h is -2.17 ± 0.17 and indicates westward propagation with zonal wavenumber 2.

The window size used to obtain the above three spectral components is too large (45 days) to prove that these waves, or at least two of them, occur simultaneously. However, the strong 2-day wave amplitude modulations, shown in Fig. 4, take place between June 30 and July 25 for most of the sites. If we assume that two of the above three different 2-day wave components occur simultaneously in July, we would be able to explain the global-scale amplitude modulations with periods ~ 9 –10 and 14–17 days present in Fig. 4. If there is a beating between the waves with periods 42.5- and 48.5-h, this would provide the amplitude modulation with period ~ 14.5 days. Such modulation is evident at almost all sites shown in Fig. 4. If the beating occurs between the waves with periods 42.5 and 52.5 h the amplitude modulation of the 2-day wave in the zonal wind should have a period of 9.3 days. The amplitude modulation with period ~ 9 –10 days is evident at Obninsk, Collm, Durham and Yamagawa. If the beating, however, takes place between the waves with periods 48.5 and 52.5 h the observed amplitude modulation should have a period ~ 23 –24 days. The interval of PSMOS campaign (3 months) is not long enough to obtain information about the amplitude modulations with period longer than 20 days. However, a few sites that have regular measurements for 1999 supplied data for the whole year. Fig. 7 is analogous to Fig. 4, however, the wavelet spectra are calculated up to a period of 30 days and the analysed interval of data for the four stations is 8 months, between March 01 and October 31, simply to avoid the winter 2-day wave activity. The figure shows that at all stations the amplitude modulation consists of too broad band of periods, but the basic response is around 14–15 and 23–27 days. We therefore conclude that at least two waves are occurring simultaneously in July at all sites, where the 2-day wave amplitude modulation is well evident (Fig. 4).

In the second half of August, a moderate burst with period longer than 60 h is evident in Fig. 5 for some stations. This oscillation is easily obtained by the correloperiodogram analysis and the amplitude spectra of six sites where this oscillation is significant are shown in the upper panel of Fig. 8. The zonal wavenumber of this wave obtained on the basis of the longitudinal dependence of the derived phases was found to be very close to 3. We have to mention that

frequently the 2-day wave activity, especially over Europe, demonstrates a final burst with large period, approaching sometimes 2.5–3 days (Pancheva et al., 2000).

3.2. 2-day wave activity in the meridional wind

A similar analysis was performed for the meridional wind. We will start again with the variability of the 2-day wave amplitudes obtained by the complex demodulation method. In this case the results are divided into amplitude modulations observed over Europe and the result is shown in Fig. 9a, and modulations over North America and Asia, presented in Fig. 9b. Manson et al. (2004) using CUJO (Canada US Japan Opportunity) network of mid- and high mid-latitude MF radars also showed that the changes of the wave amplitudes with longitude are very significant and often exceed the changes with latitude. Fig. 9a demonstrates some latitudinal dependence of the modulations over Europe. At high latitudes the 15-day modulation is predominant, while the 8–10-day modulation can be seen at middle latitudes. The North American mid-latitudes sites indicate very similar behaviour; strong amplitude modulation with period ~ 14 –15 days, as only Saskatoon shows slightly longer period of 17 days (however, the Saskatoon data set has a relatively long gap of 11 days just at the central part of the 2-day wave activity that surely affects this result). The modulation at Urbana is the strongest and its amplitude reaches 12 m/s (note that this is the variability of the 2-day wave amplitude, not the amplitude itself). The behaviour of the 2-day wave amplitude variability at Yamagawa is similar to those for the North American sites, while a modulation with period 13–15 days can be seen at Hawaii as well, but slightly earlier. Figs. 9a and b show that, similar to the zonal component the main variability of the 2-day wave amplitudes in the meridional component is again mainly in the second half of June and July, while it is very weak or almost absent in August.

To study the 2-day wave bursts we again perform the wavelet transform on the hourly meridional wind data in the period range between 30 and 72 h and the result for all sites is shown in Fig. 10 (the stations are arranged in the same way as in Fig. 5). For most of the sites the 2-day wave activity amplifies between June 20 and July 31, while a separate 2-day wave burst with an increasing period is evident in many stations during August. Again observing carefully at the 2-day wave bursts occurring simultaneously at most of the sites in the interval between June 20 and July 31 we cannot determine some predominant spectral components. For example, the burst centred at July 16 has period close to 48 h at Urbana, Durham and London, while at European stations it changes from 40 to 54 h. This could

Fig. 5. The wavelet transform of the hourly values of the zonal wind in the period interval 30–72 h, performed for all sites shown in Fig. 1 (except Collm, as we have only 6-hourly amplitudes of the 2-day wave). The results are arranged in the same way as in Fig. 1 starting from Resolute Bay (the upper left figure) and ending at Hawaii (the lower right figure).

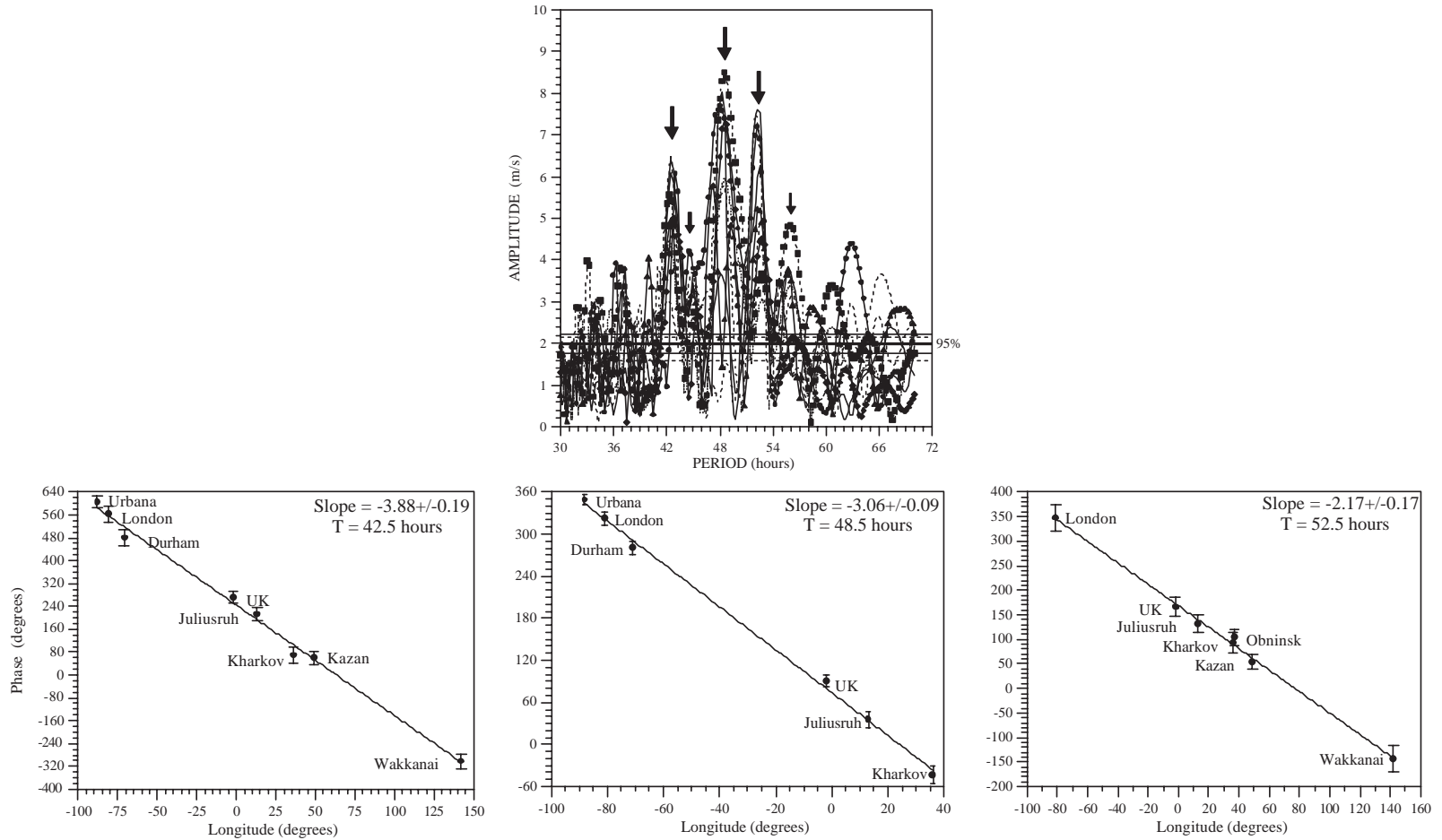


Fig. 6. The upper plot shows the amplitude spectra calculated for the period interval 30–70 h for the zonal wind in the interval 25 June–10 August, 1999 measured at Castle Eaton (thick solid), Juliusruh (thick dashed), Kharkov (thin solid), Obninsk (thin dashed), Kazan (thick solid with dots), London (thin solid with diamond), Wakkanai (thin solid with triangle), Urbana (thick dashed with squares) and Durham (thin dotted); the 95% confidence levels for all sites are shown also. Big arrows mark the three main peaks situated at: 42–43, 48–49 and 52–53 h, while small arrows mark the weaker peaks around 45 and 55 h. The lower panel plots show the phase distribution as a function of longitude for the waves with periods: 42.5 h (left plot), 48.5 h (middle plot) and 52.5 h (right plot).

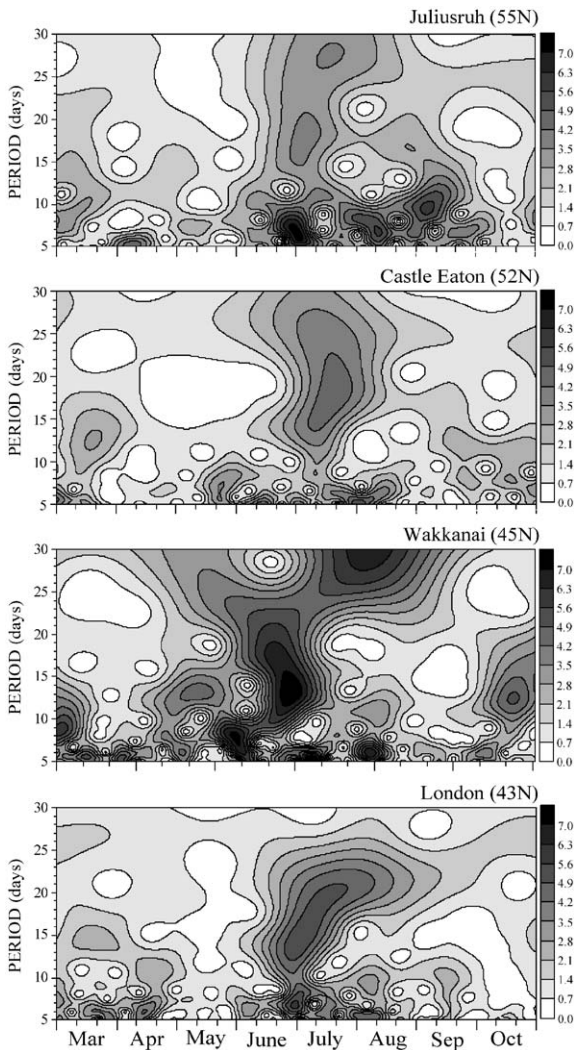


Fig. 7. The wavelet transform of the hourly values of the amplitudes of 2-day wave in the zonal wind (obtained by complex demodulation) at four stations, Juliusruh, UK, Wakkanai and London, performed in the period range 2–30 days and for the interval 01 March–31 October 1999.

be a result from the simultaneous occurrence of more than one wave that composed the 2-day wave bursts during June 30–July 31. To study the main quasi-2-day periodicities in this interval we again use correlogram analysis.

The upper plots of Fig. 11 show the amplitude spectra derived from the hourly mean meridional winds measured between June 20 and July 31, for all sites that have at least one full month of continuous measurements. The amplitude spectra for Europe (left panel) and for North America and Asia (right panel) demonstrate some slight differences and that is why they are shown in separate panels. Similar to the zonal wind, three main peaks, marked by arrows, are clearly

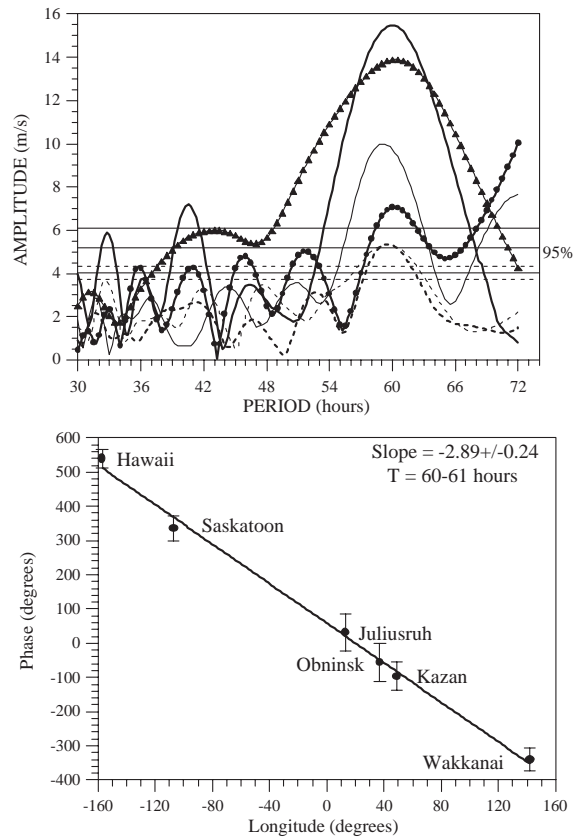


Fig. 8. The amplitude spectra (upper plot) in the period interval 30–70 h for the zonal wind in the interval 10–31 August, 1999 measured at Hawaii (thick solid), UK (thick dashed); Saskatoon (thin solid), Kharkov (thin dashed), Wakkanai (thin solid with triangle) and Kazan (thick solid with dots); the 95% confidence levels for all sites are shown also. Phase distribution as a function of longitude for the wave with period 60–61 hours (bottom plot). The wave phase is in degrees, with $0^\circ = 0$ UT.

evident in the meridional wind as well. The first two peaks are identical for Europe and North America, while a slight difference is found for the peak with the longest period. The first two peaks are centred around 42–43 and 50 h, while the third one for Europe is centred at 54–55 h and for America and Asia—at 56–57 h.

The zonal structure of these spectral components is obtained again by a least-squares best-fit procedure applied to the time interval under consideration. The results are shown in the lower panel plots of Fig. 11 and they are similar to those for the zonal component. The left plot shows the longitudinal dependence of the derived phases of the oscillation with an average period of 43 h for the various sites. The slope of the fitted line obtained by a weighted least-squares best-fit line is -3.98 ± 0.11 , and this indicates a westward-propagating wave with a zonal wavenumber 4. The slope of the second spectral component (middle plot)

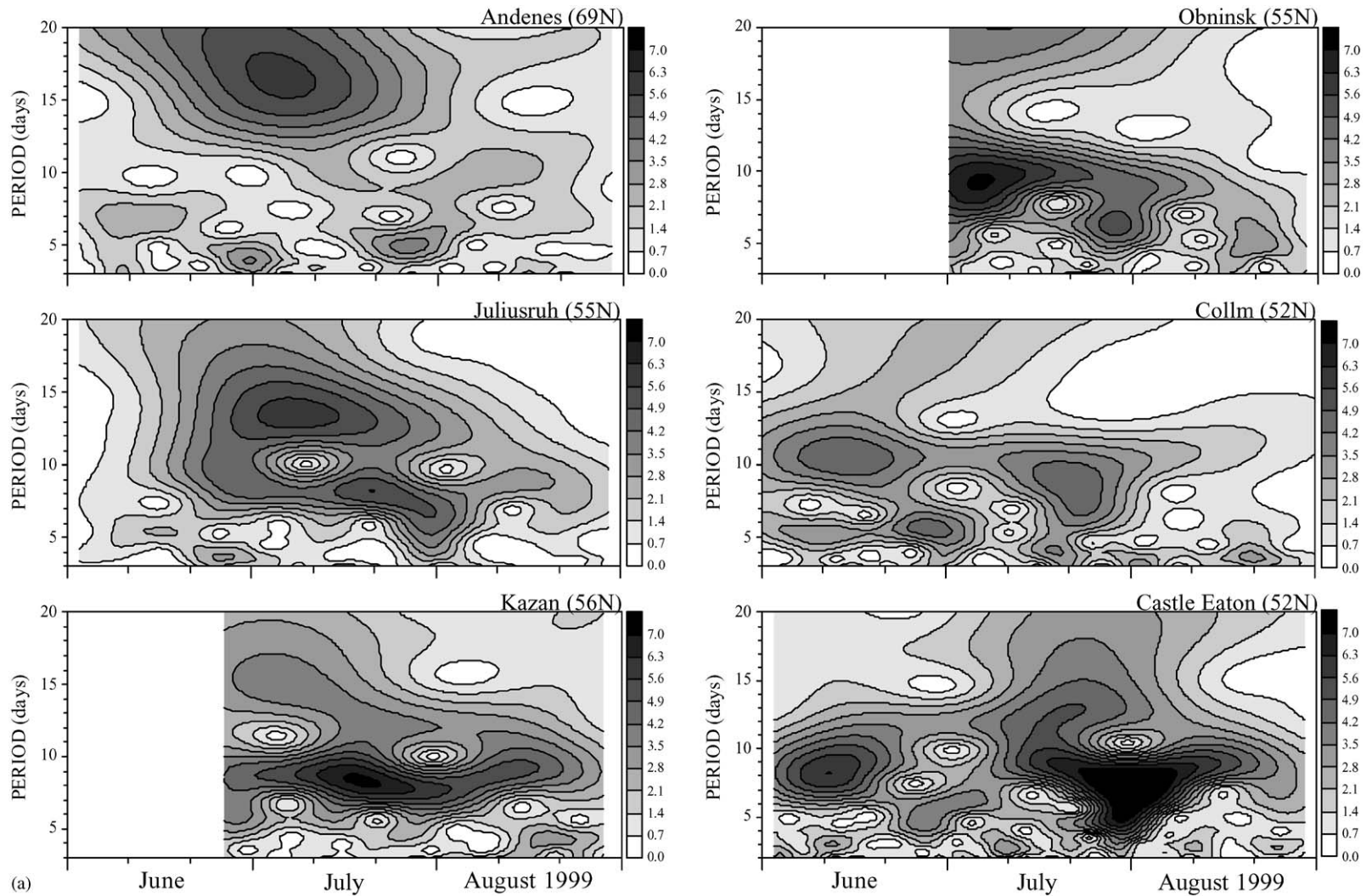


Fig. 9. (a) The wavelet transform of the hourly values of the amplitudes of 2-day wave in the meridional wind (obtained by complex demodulation) at six European stations arranged according to their latitudes, starting from upper right with the most northern station Andenes (69°N) and finishing at the lower left with the most southern one Castle Eaton (52°N). (b) The same as in Fig. 9a, but for the six North American and Asian sites, marked at the upper right edge of each plot.

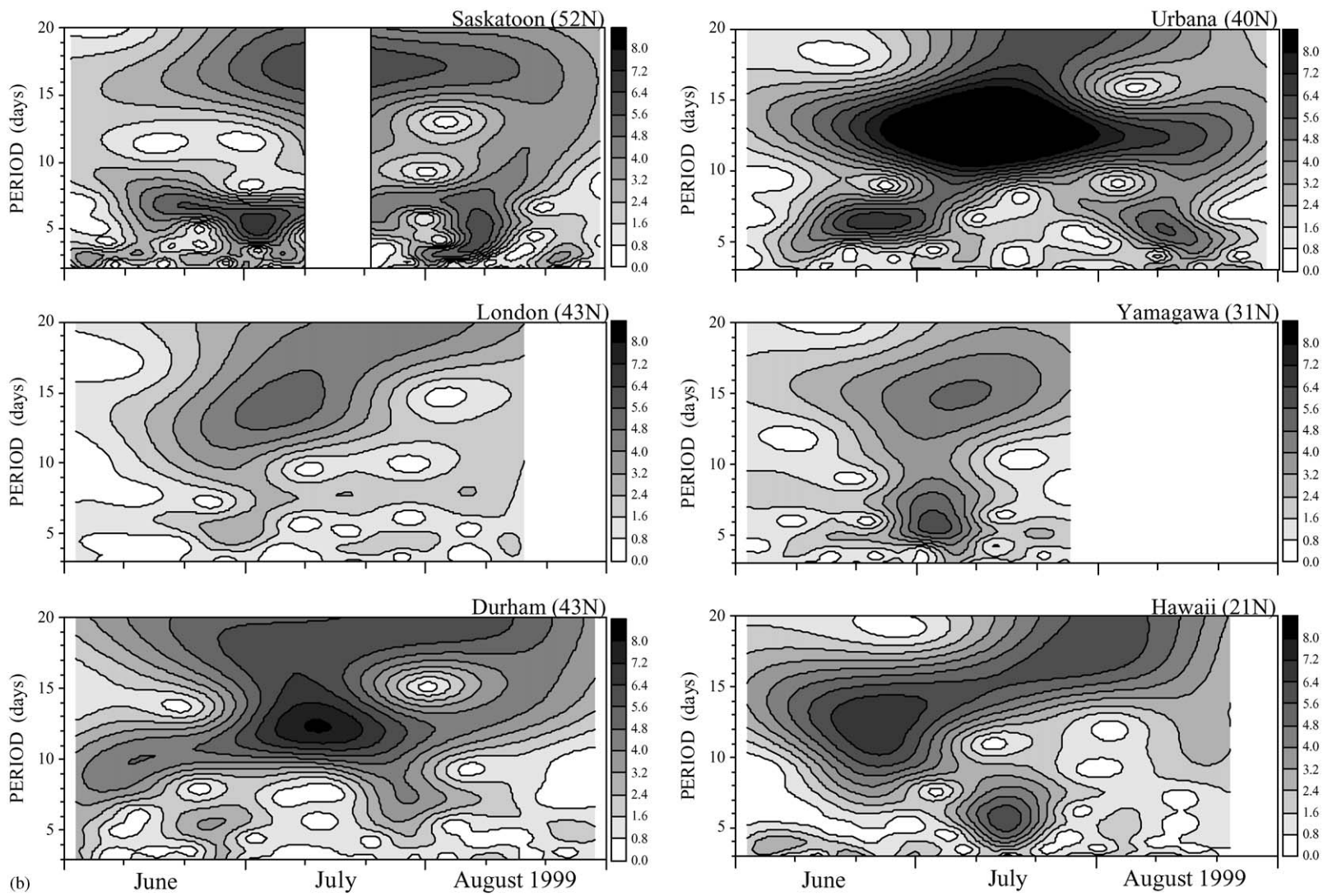


Fig. 9. *continued.*

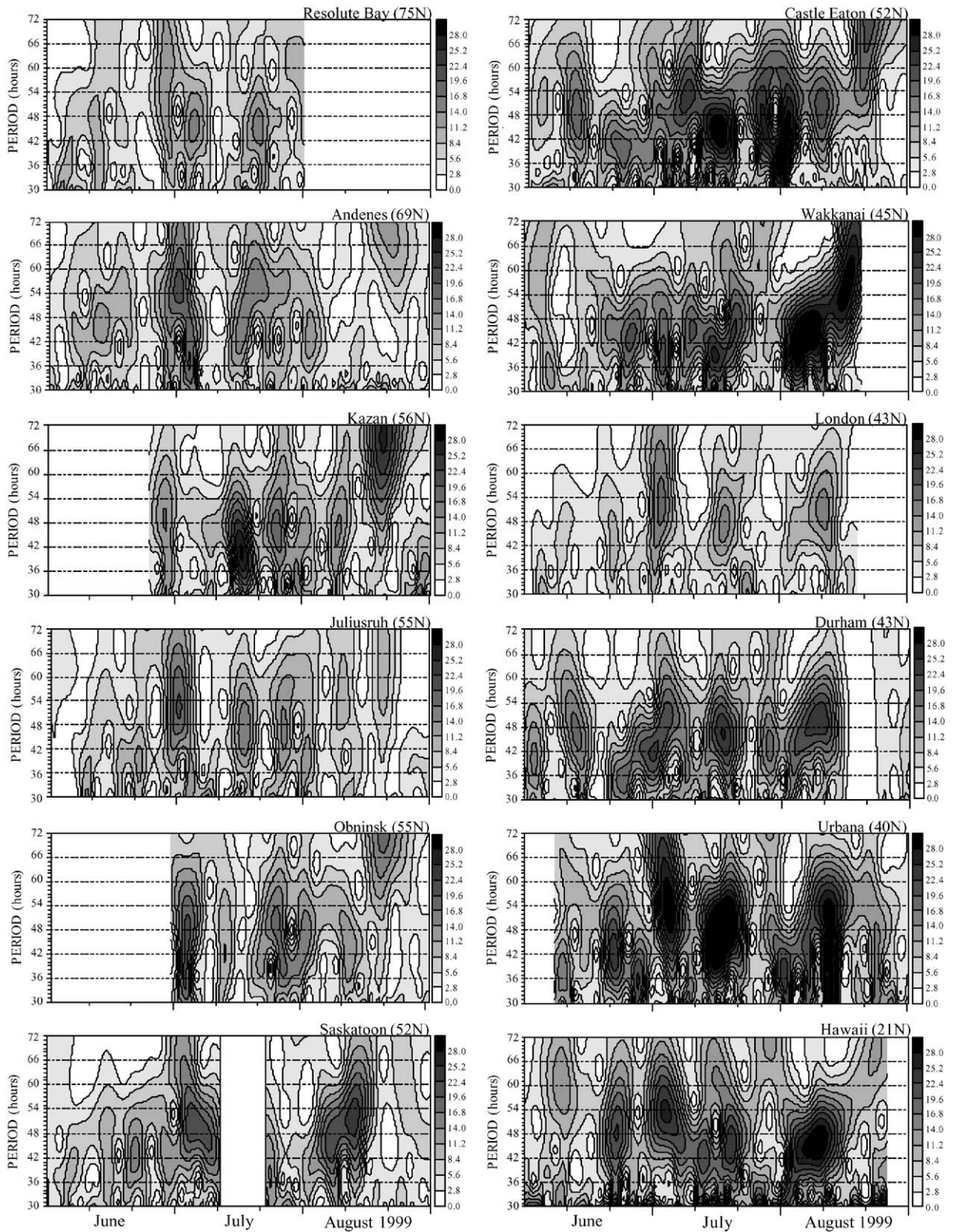


Fig. 10. The same as Fig. 5, but for the meridional wind.

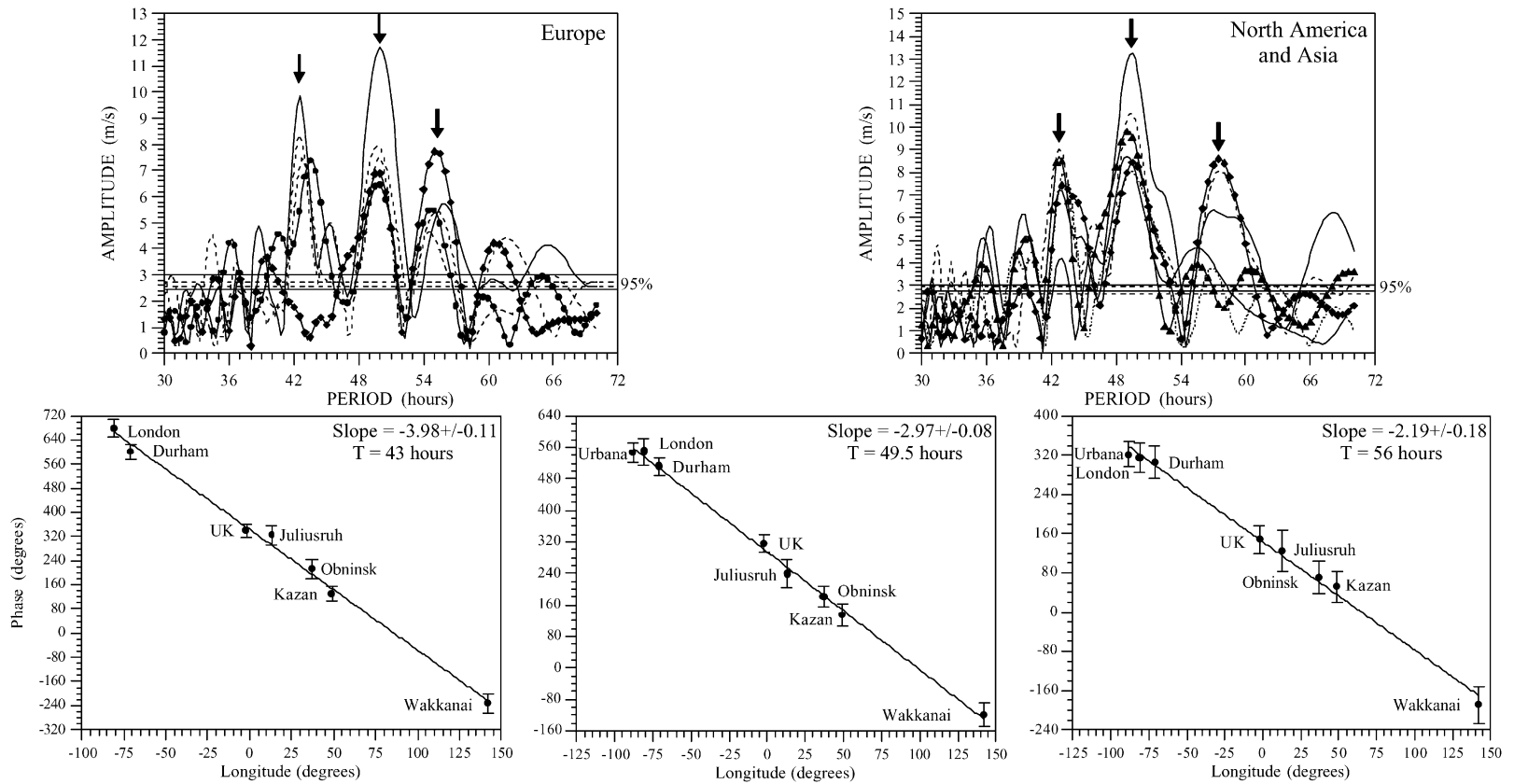


Fig. 11. The upper panel of plots show the amplitude spectra in the period interval 30–70 h for the meridional wind in the interval 20 June–31 July, 1999 measured at the European stations (left plot): Castle Eaton (thick solid), Juliusruh (thick dashed), Obninsk (thin dashed), Andenes (thin solid with diamond) and Kazan (thick solid with dots). And at the North American and Asian stations (right plot): Urbana (thick solid), Hawaii (thick dashed), Yamagawa (thin solid), Durham (small dashed), London (thin solid with diamond) and Wakkanai (thin solid with triangle). The lower panel of plots show phase distribution as a function of longitude for the waves with periods: 43 h (right plot), 49.5 h (middle plot) and 56 h (right plot). The wave phase is in degrees, with $0^\circ = 0$ UT.

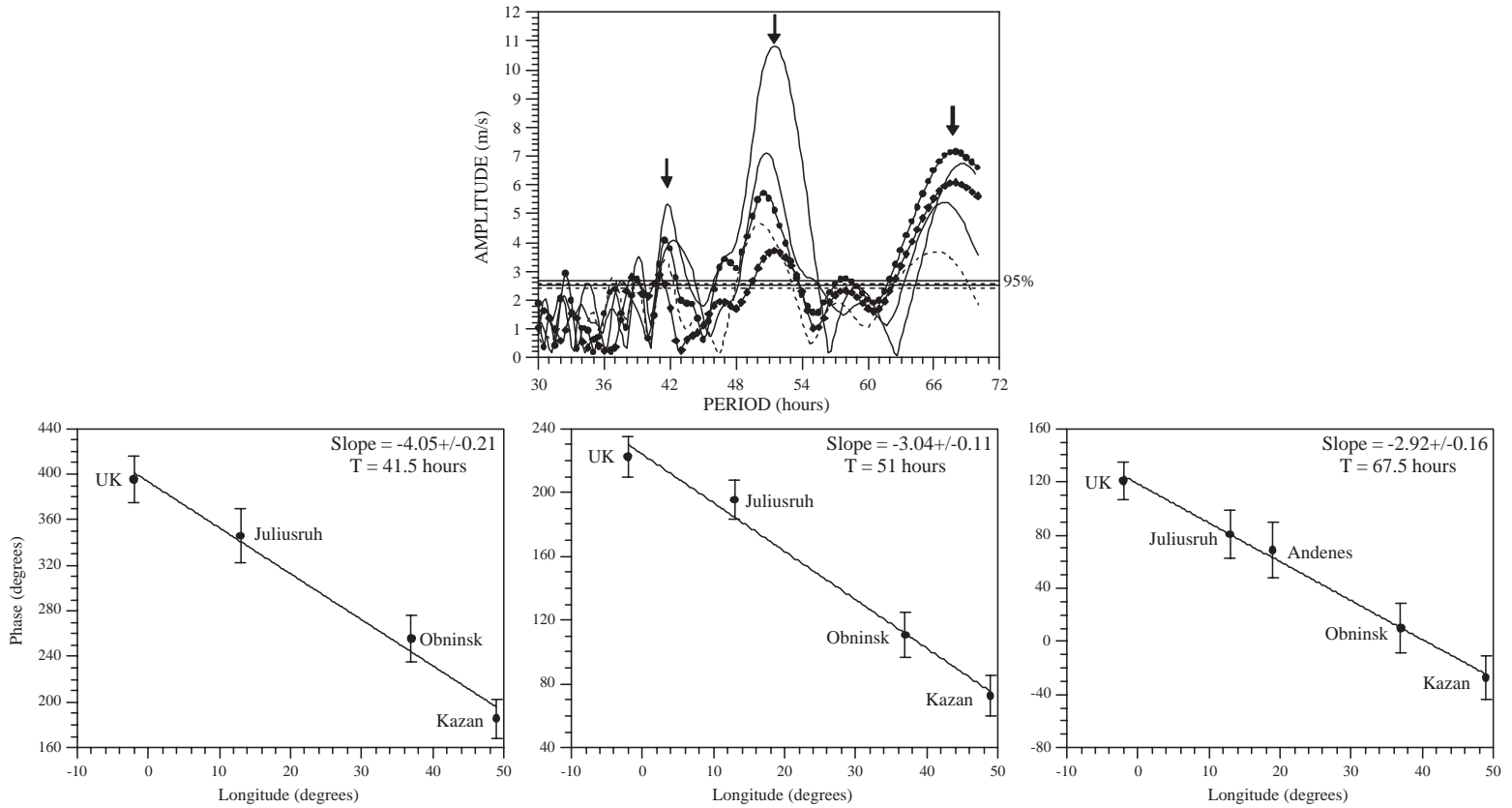


Fig. 12. The upper plot shows the amplitude spectra in the period interval 30–70 h for the meridional wind in the interval 31 July–31 August, 1999 measured at the European station: Castle Eaton (thick solid), Obninsk (thin solid), Juliusruh (thick dashed), Andenes (thin solid with diamond) and Kazan (thick solid with dots). The lower panel of plots shows phase distribution as a function of longitude for the waves with periods: 41.5 h (left plot), 51 h (middle plot) and 67.5 h (right plot). The wave phase is in degrees, with $0^\circ = 0$ UT.

with an average period of 49.5 h is -2.97 ± 0.08 , and it indicates a westward-propagating wave with a zonal wavenumber of 3. The slope of the third spectral component (right plot) with a mean period of 56 h is -2.19 ± 0.18 and indicates westward propagation with zonal wavenumber 2.

As was the case with the zonal wind, the window used here was too large (42 days) to prove that these three waves, or at least two of them, occur simultaneously at most of the sites. Again however, we come back to the strong 2-day wave amplitude modulations observed in July with some exceptions at Collm, Castle Eaton and Hawaii, where the variability of the 2-day wave amplitude is evident in June as well (see Figs. 9a and b). If we assume that two of the above three different 2-day wave components occur simultaneously in July, we would be able to explain the global-scale amplitude modulations with period ~ 8 –10 and 14–17 days observed in Figs. 9a and b. If the beating occurs between the waves with periods 43- and 49.5-h we may observe the amplitude modulation with period ~ 13.6 days. A similar modulation is evident at all North American sites shown in Fig. 9b. If the beating takes place between the waves with periods 43 and 54–55 h the amplitude modulation of the 2-day wave in the meridional wind has to have period of 8.5 days, and similar modulation can be seen in Europe for latitudes not higher than 55°N . If the beating is between the waves with periods 49.5 and 56 h, the observed amplitude modulation has to have a period of ~ 17.5 days. Similar modulations can be seen over Saskatoon, Hawaii, Yamagawa and Andenes.

The 2-day wave activity in the meridional wind during August is especially strong over North America and Asia, while the long lasting burst over Europe has a period larger than 2.5 days, similar to the zonal component (see Fig. 10). The calculated amplitude spectra for the time interval 1–31 August show similar periods only for European sites. The European spectra are presented in Fig. 12 (upper plot), where the strongest peak has a period of 51 h. There is also a weak peak at 41–42 h and the final 2-day wave peak at 67–68 h. Their zonal wavenumbers are presented in the lower panel plots of Fig. 12 and they are 4, 3 and again 3 for the mean periods 41.5, 51 and 67.5 h, respectively. If we consider carefully the 2-day wave bursts in August (see Fig. 10), we can clearly distinguish an increase of the period with time. Actually, there are two bursts centred at August 10 and 20. The first of them has different peaks at wavelet spectra for many of the European stations, changing from 41 to 51 h, while the second burst at all sites has period of 67–68 h and it corresponds to the third peak evident in the upper plot of Fig. 12. This means that only the first burst, centred at August 10, could be composed of two spectral components with periods of 41–42 and 51 h.

Looking at the four stations in Fig. 10, we can clearly distinguish two bursts with almost the same periods: about ~ 45 and 51 h, as the shorter period is not evident well in all sites. The presence of these oscillations in most of the North American and Asian sites is documented by the cross-wavelet analysis shown in Figs. 13a and b. The zonal

structure of these oscillations is determined by the phase difference between different pairs of stations (obtained by cross-wavelet transform). We obtained a zonal wave number close to 4 for the shorter period oscillation (44–46 h) and zonal wavenumber 3 for the 50–52 h one. Therefore, the 2-day wave activity in August over North American and Asian sector is composed of two spectral components. The 44–46-h burst is centred around August 6–7, while the 50–52-h burst—around August 12–13.

4. Discussion

As part of PSMOS project a campaign of measurements was conducted during June 1 and August 31, 1999 using a large number of MLT-region radars. The neutral wind measurements from 15 radars situated in the Northern Hemisphere have been combined to analyse the global-scale structure of the quasi-2-day wave during this summer period. In general, the 2-day wave activity in the northern summer of 1999 was not exceptionally strong, but the wave was well evident in both zonal and meridional wind components. We were not able to study in detail the vertical features of this wave because only data for two altitude levels were provided (~ 90 and ~ 95 km). In spite of this, we used this information for investigating the altitude variability of the 2-day wave amplitudes at least in this height range of 90–95 km. The behaviour of the 2-day wave amplitudes at both levels was found to be very similar with only a slight tendency for the amplitudes to decrease with height. The latitudinal variability of the 2-day wave indicated some amplification in the middle and high-middle latitudes (Fig. 3). However, we have to notice that most of the radars were situated in this latitudinal range.

The day-to-day variability of the 2-day wave amplitudes was found to be significant. The global-scale amplitude modulations with periods 8–10 and 14–17 days were evident mostly at the end of June and July, while in August they were almost absent. This observational result was the reason for studying the 2-day wave activity separately for both intervals (or for the interval with and without observed amplitude modulations).

The 2-day wave activity during the end of June/July was in fact composed of three westward propagating waves with zonal wave numbers 4, 3 and 2. The periods associated with these wave numbers were, respectively, 42–43, 48–50 and 53–56 h. We noticed that these three spectral components were found at most, but not at all sites. The simultaneous presence of at least two spectral components with periods close to each other is a key result that may serve to explain the observed amplitude modulations by beating between different spectral components.

The 2-day wave activity in August demonstrated some difference between the zonal and meridional components. Only one final burst with period 60–61 h and westward propagation with zonal wave number 3 was observed in the

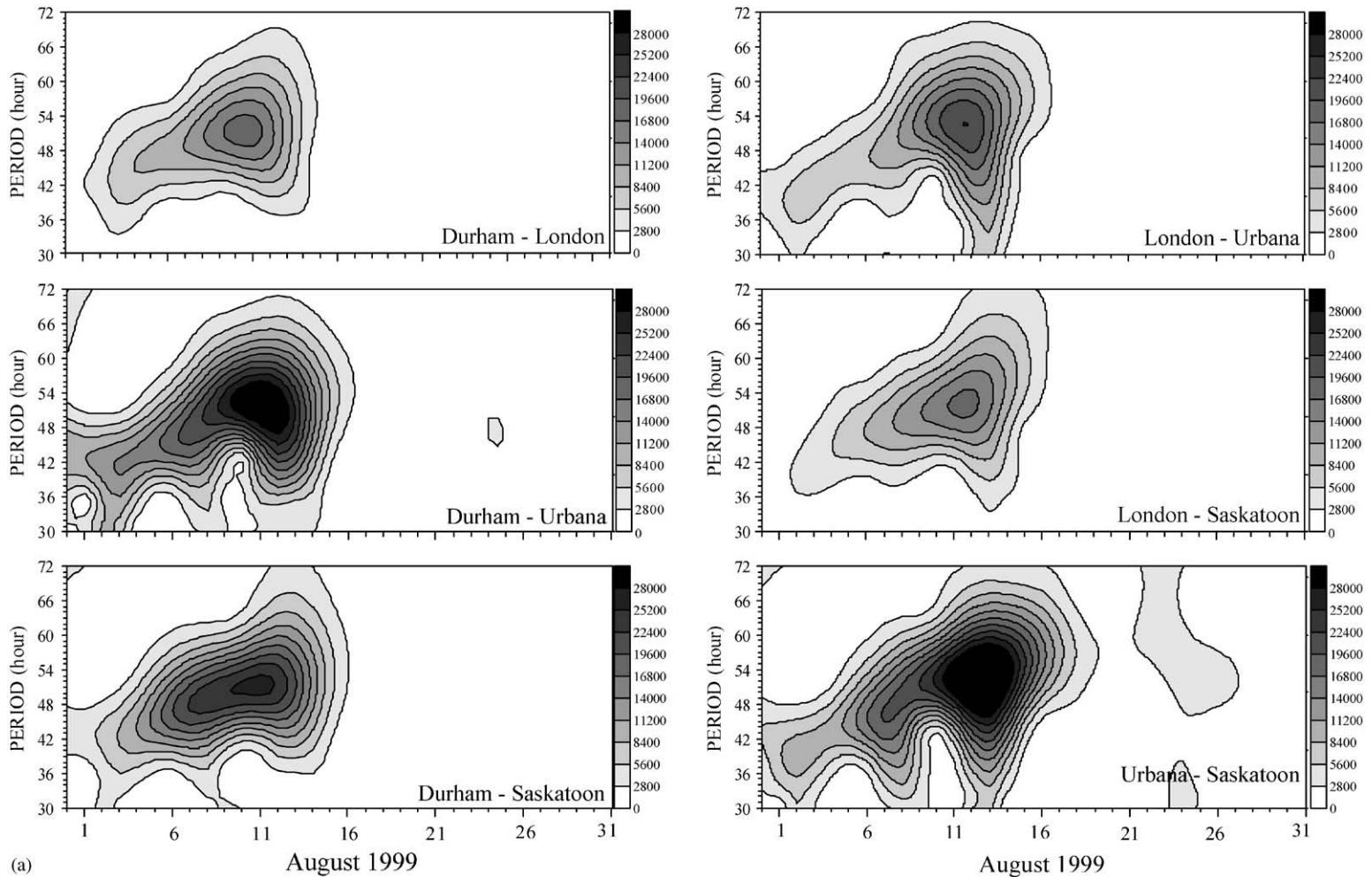


Fig. 13. (a) Crosswavelet spectra obtained from the hourly values of the meridional wind measured in the interval 31 July–31 August, 1999 at the indicated pairs of North American stations. (b) The same as Fig. 13a, but at indicated pairs of North American and Asian stations.

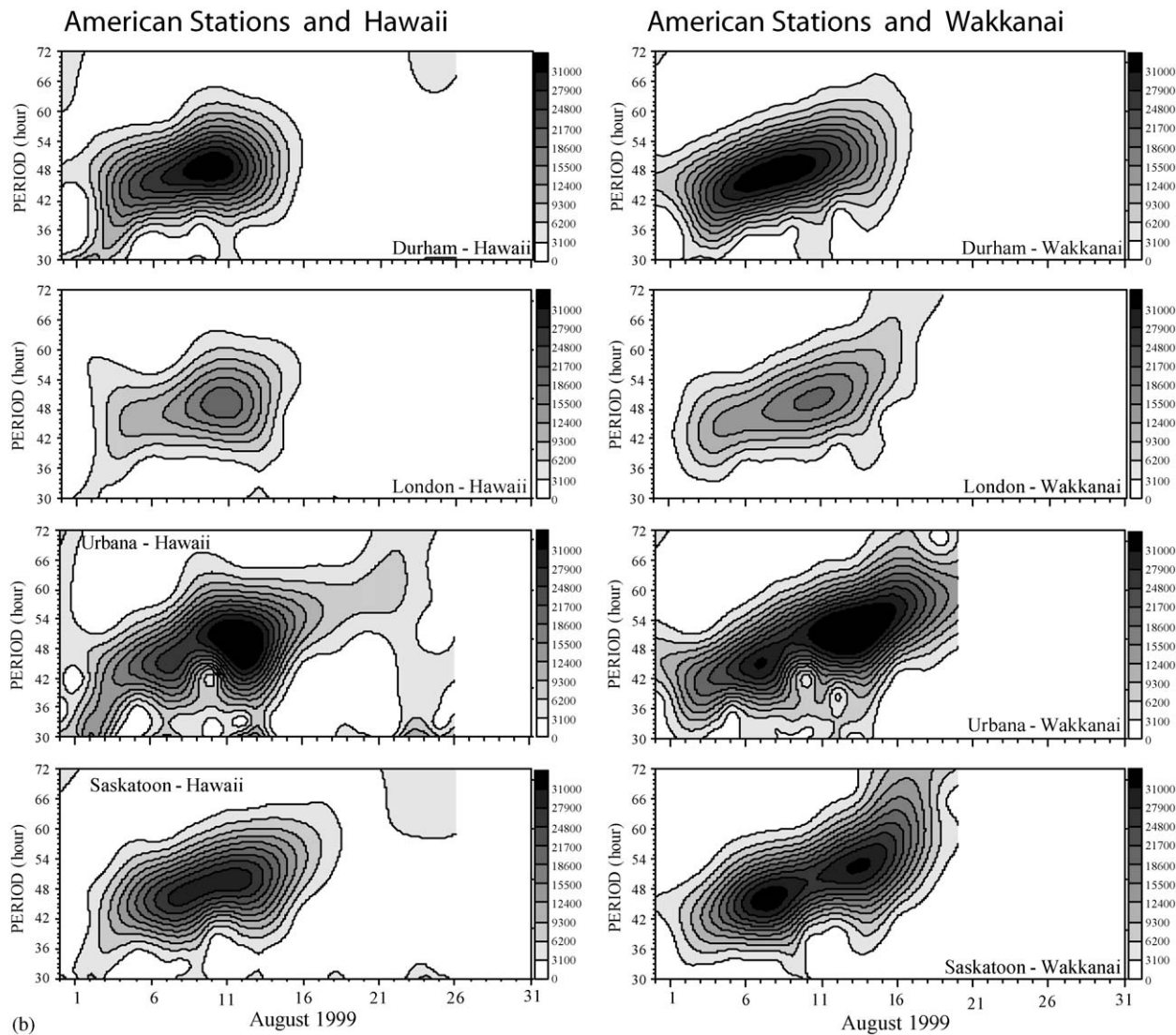


Fig. 13. *continued.*

zonal wind and at most of the sites. Two significant spectral components however, were found in the meridional wind and some difference between Europe and North America was revealed. Over Europe we found waves with periods ~ 50 – 51 and 67 h and both of them were westward propagating with zonal wave number 3. The important fact is that these components probably do not occur simultaneously; first the 50 – 51 -h wave was observed (weakly influenced by the 41 – 42 -h wave) and later the 67 -h wave that actually completed the 2-day wave activity in the northern Summer 1999. A similar behaviour in the 2-day wave activity was observed over North America and Asia in August. First, the wave with period 44 – 46 h and zonal wavenumber close to 4 was evident in some sites and shortly after that a wave with period 50 – 51 h and zonal wavenumber 3 was found. The successive presence of the observed spectral components in the meridional wind in August is a probable reason that could explain the absence of the amplitude modulations.

An important question in this study is: *what is the mechanism of generating these spectral components that composed the 2-day wave activity in the northern Summer 1999?* The simultaneous presence of several spectral components that compose the 2-day wave activity most probably is related to the instability hypothesis for the generation of the 2-day wave. In the two-dimensional model of Pfister (1985) unstable responses for zonal wave numbers between 2 and 4 with periods between 1.5 and 3 were found. Analysing the HRDI wind and temperature data for January 1994, Lieberman (1999, 2002) showed that the 2-day wave episode was actually a wave “packet” composed of zonal wave numbers 4, 3 and 2 that propagated westward with a phase speed near 60 m/s. The periods associated with these zonal wave numbers were 1.7, 2.1 and 3.5 days, respectively. She found also that all three waves are characterized by baroclinic structure.

Observational support of the instability hypothesis has to reveal the generation of the 2-day wave in the presence of negative gradients of zonally averaged potential vorticity. From the PSMOS data base we cannot perform such kind of analysis because of lack of required data. An indication for the validity of the instability mechanism is the generation of a wave packet. This means that the waves have to have the same phase speed. In our case only the 42 - and 50 -h waves have similar (but not the same) phase speeds, 0.9 – 1 rad/day, while the phase speed of the 55 -h wave was higher, 1.37 rad/day.

If we consider carefully the evolution in time of the spectral components that composed the 2-day wave activity in the northern Summer 1999 an interesting fact can be revealed. Fig. 14 shows the amplitude spectra obtained by moving short-time (or windowed) Fourier transform (the length of window is 720 h transferred in steps of 24 h) for stations without long gaps. Although the Fourier transform spreads information about the localized features over all scales we can notice that the 2-day wave activity, especially in the zonal component, started with a 48 -h wave and later,

when the 30-day window is centred at the end of June and July the other periods appear as well. Analysing the tidal variability and its possible relationship to the coupling with the planetary waves during the PSMOS campaign Pancheva et al. (2002b) found a 16-day wave (actually, the detected period in different sites changed between 14 and 17 days) that showed some amplification in the end of June/July. A possible non-linear interaction between the (3,0) Rossby-gravity mode and the 14 – 17 -day planetary wave can generate secondary waves with periods ~ 42 and 55 h. In Pancheva et al. (2002b) it was found that the 14 – 17 -day wave is westward propagating with zonal wavenumber 1. Then, the generated secondary waves have to have zonal wave numbers 4 for the 42 -h wave and 2 for the 55 -h wave. Such waves we have already found, as the 42 -h wave was evident in both zonal and meridional components (see upper plots of Figs. 6 and 11), while the 55 – 56 -h wave was evident mainly in the meridional wind (upper plot of Fig. 11), but there is a peak in the zonal component as well (marked by small arrow in the upper plot of Fig. 6). In the zonal wind however, we found a wave with shorter period 52 – 53 h. Such a wave could be generated from the coupling between the Rossby-gravity mode and the planetary wave with period 24 – 26 days.

The observed 14 – 17 -day planetary wave could affect the (3,0) Rossby-gravity mode through the change of the background conditions, as the PW may perturb the background zonal wind and temperature fields. Hagan et al. (1993) demonstrated that the shifts in resonance period of the 2-day wave as well as the differences in the magnitudes of the resonant responses are wholly attributable to the differences in the background zonal wind. They noted also that the changes in the summer lower thermosphere jet could set up a reflecting layer that leads to an enhancement of the mesospheric wave signature. Therefore, the periodic modifications in the background conditions by the 14 – 17 -day planetary wave could inhibit or enable propagation of the 2-day wave in the lower thermosphere. Then the observed amplitude modulation with period ~ 14 – 17 days could be explained by the refractive influence caused by the disturbed background fields on the (3,0) Rossby-gravity mode. This explanation is similar to the mechanism proposed by Riggin et al. (2003) for the modulation of the semidiurnal tide with periods of the planetary wave. In this study however, we found that the spectral components composing the 2-day wave activity have different zonal structure. This complex picture cannot be explained by Hagan et al. (1993) or Riggin et al. (2003) results.

In order to investigate the possible non-linear effects in the neutral wind we apply bispectral analysis to the hourly wind measurements. In the present work, the magnitude-squared bispectrum is calculated (Pancheva, 2000) that is based on the division of the time series into overlapping segments. To obtain a statistically representative result we need to have enough segments and this condition requires longer time series. We mentioned before that a few sites that have

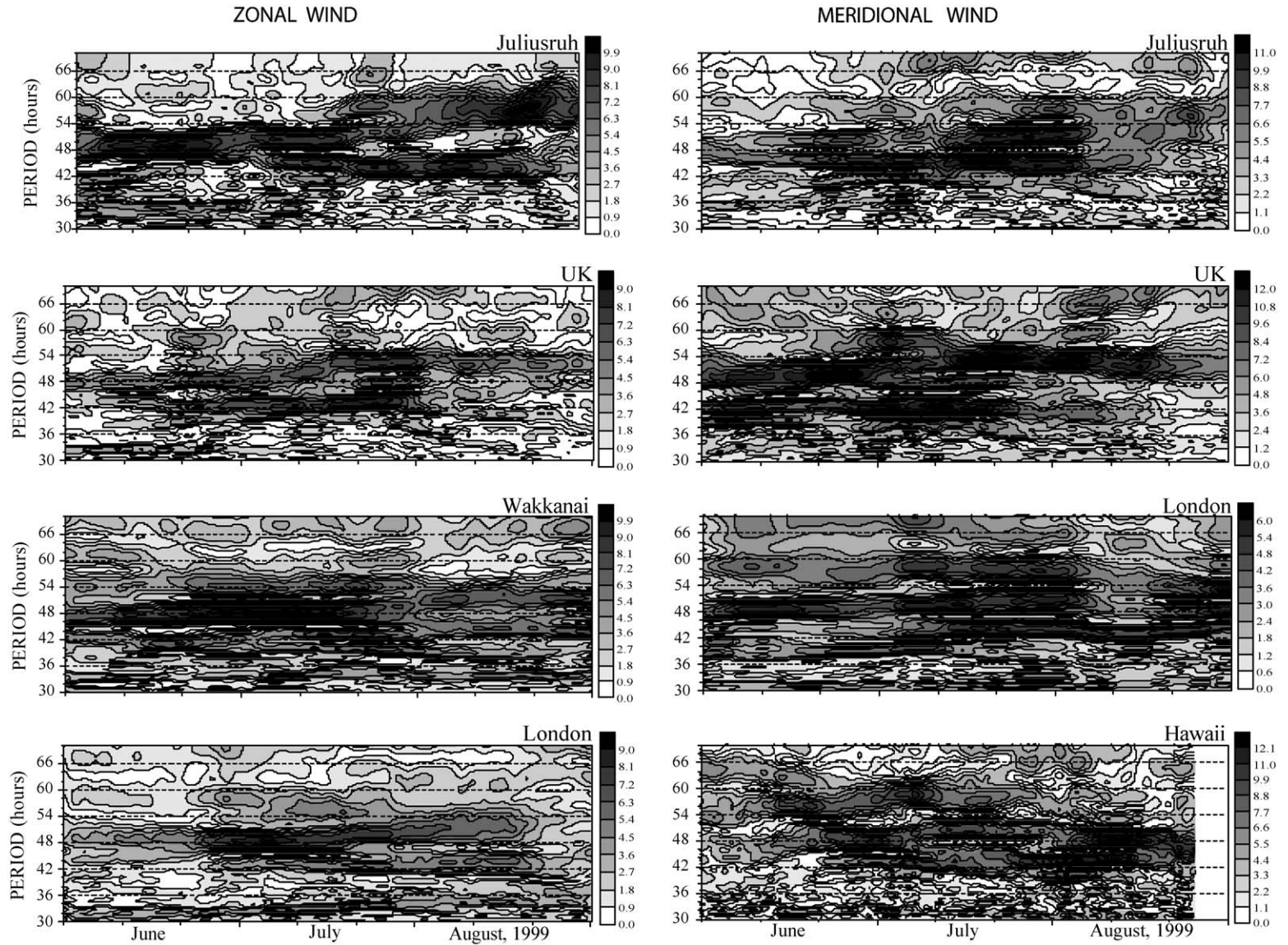


Fig. 14. The amplitude spectra obtained by moving short-time (or windowed) Fourier transform (the length of window is 720 h transferred through the time series in steps of 24 h) for stations without long gaps. The names of the stations are indicated at the right upper edge of each plot.

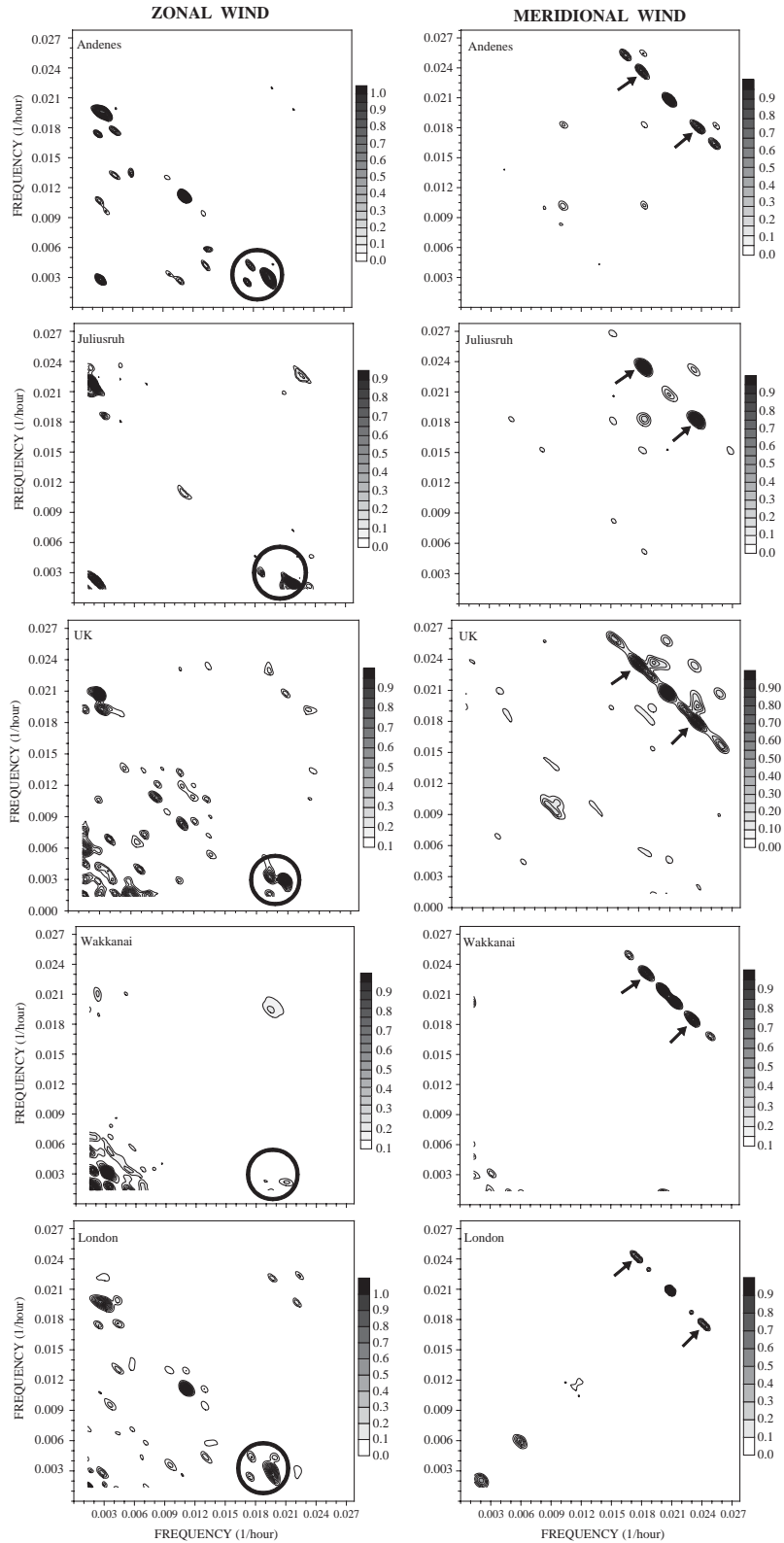


Fig. 15. Magnitude-squared bispectra calculated in the period interval 30–720 h from the hourly values of zonal (left column) and meridional (right column) winds measured during the interval 01 March–31 October, 1999. The strongest interactions in the zonal wind are marked by circle, while those in the meridional wind—by arrows.

regular measurements provided data for the whole year 1999. Using the data for the interval March 1–October 31, which include only the summer 2-day wave activity, we calculated the magnitude-squared bispectrum. The result is shown in Fig. 15, where the plots in the left column are for the zonal wind and the plots in the right column are for the meridional wind. We immediately notice that the bispectra for the zonal and for the meridional winds are very different. The strongest interactions in the zonal wind are between the spectral components that compose the 2-day wave activity and the other planetary waves, as well as between different (other than 2-day wave) planetary waves. In the meridional wind however, the strongest interactions are those between the spectral components that compose the 2-day wave activity.

If we consider carefully the plots in the left column all interactions marked by a circle (right bottom part of the panel) indicate the coupling between the spectral components that composed the 2-day wave (with frequencies between 0.017 and 0.021 cycles/h) and ~ 14 –15- (or frequency 0.0028–0.003 cycles/h) and 22–25-day (or frequency 0.0017–0.002 cycles/h) planetary waves (with an exception Wakkanai that shows interaction only with a 20–22-day planetary wave). This result gives some evidence for a possible coupling between the 2-day wave and the longer period planetary waves. Some additional evidence that supports the non-linear interaction between the Rossby-gravity mode and the 25-day planetary wave is the presence in the spectra of the sum-secondary wave as well. This wave has to have a period of about 45 h. If we consider carefully the spectra shown in upper plot of Fig. 6 this peak is evident there and it is marked by a small arrow (left peak). The right peak marked by a small arrow, situated at 55–56 h and visible only at some sites, is a difference secondary wave that is generated by the coupling between the 48–49-h wave and 15-day planetary waves.

The interactions marked by arrows in the right column panels of Fig. 15 indicate coupling between ~ 42 –43 (frequency 0.023–0.024 cycles/h) and 55–56-h (frequency 0.018–0.0182 cycles/h) waves found in the meridional wind. The third wave participating in this interaction (a sum-secondary wave) is actually a wave with period very close to 24 h, but its zonal wave number should be 6. Therefore, this wave could be a non-migrating diurnal tide with zonal wave number 6. This tide has been hypothesized to be the mechanism for locking the quasi-2-day wave to local time and to the sudden increase in the 2-day wave amplitudes that has been frequently observed (Walterscheid and Vincent, 1996). These authors suggested two possible cascades for the generation of this non-migrating tide that involve large-amplitude migrating semidiurnal and diurnal tides. In our case this tide could be generated directly by the coupling between the ~ 42 –43 and 55–56-h waves that have the zonal wave numbers 4 and 2, respectively.

5. Summary

The neutral wind measurements from 15 radars situated in the northern hemisphere between latitudes 21°N and 75°N and longitudes 142°E and 157°W were combined to analyse the global-scale structure of the quasi-2-day wave activity during the northern Summer 1999. The day-to-day variability of the 2-day wave amplitudes was found to be significant. The global-scale amplitude modulations with periods 8–10 and 14–17 days were evident mostly in July, while in June and August they were almost absent. The 2-day wave activity in June was weak, composed mainly by a 48-h wave. The successive presence of the two bursts with periods ~ 45 and ~ 51 h in the meridional wind over North America and ~ 51 and ~ 67 h over Europe in August is a probable reason the amplitude modulations to be almost absent. The 2-day wave activity in July was in fact composed of three westward propagating waves with zonal wave numbers 4, 3 and 2. The periods associated with these wave numbers were 42–43, 48–50 and 53–56 h, respectively. The simultaneous presence of at least two spectral components with periods close to each other is a key result that may serve to explain the observed amplitude modulations by beating between different spectral components. From the planetary wave analysis of the PSMOS campaign Pancheva et al. (2002b) found a westward propagating 14–17-day wave with zonal wave number 1. A possible non-linear interaction between the (3,0) Rossby-gravity mode and the 14–17-day planetary wave can generate secondary waves with periods ~ 42 and ~ 55 h. In order to investigate the possible non-linear effects in the neutral wind, bispectral analysis was applied. The bispectra for the zonal and for the meridional wind however, turned out to be very different. The strongest interactions in the zonal wind were between the spectral components that compose the 2-day wave activity and the planetary waves with periods 14–15 and 22–25 days. In the meridional wind however, the strongest interactions were those between the spectral components that compose the 2-day wave activity (or mainly between ~ 42 –43 and ~ 55 –56 h). The third wave participating in this interaction (a sum-secondary wave) is actually a wave with frequency and zonal wave number very close to that of the non-migrating diurnal tide with zonal wave number 6. The last has been related to the locking of the quasi-2-day wave to local time (Walterscheid and Vincent, 1996).

References

- Apostolov, E.M., Altadill, D., Alberca, L., 1995. Characteristics of quasi-2-day oscillations in the foF2 at northern middle latitudes. *Journal of Geophysical Research* 100, 12163–12171.
- Beard, G.A., Mitchell, N.J., Williams, P.J.S., Kunitake, M., 1999. Non-linear interactions between tides and planetary waves resulting in periodic tidal variability. *Journal of Atmospheric and Solar-Terrestrial Physics* 61, 363–376.

- Bloomfield, P., 1976. *Fourier Analysis of Time Series: An Introduction*. Wiley, New York.
- Burks, D., Leovy, C.B., 1986. Planetary waves near the mesospheric easterly jet. *Geophysical Research Letters* 13, 193–196.
- Clark, R.R., Bergin, J.S., 1997. Bispectral analysis of mesosphere wind. *Journal of Atmospheric and Solar-Terrestrial Physics* 59, 629–639.
- Clark, R.R., Current, A.C., Manson, A.H., Meek, C.E., Avery, S.K., Palo, S.E., Aso, T., 1994. Hemispheric properties of the two-day wave from mesosphere–lower-thermosphere radar observations. *Journal of Atmospheric and Solar-Terrestrial Physics* 56, 1279–1288.
- Coy, L., 1979. A possible 2-day wave oscillation near the tropical stratopause. *Journal of the Atmospheric Sciences* 36, 1615–1618.
- Craig, R.L., Vincent, R.A., Fraser, G.J., Smith, M.H., 1980. The quasi-2-day wave in the Southern Hemisphere mesosphere. *Nature* 287, 319–320.
- Gurubaran, S., Sridharan, S., Ramkumar, T.K., Rajaram, R., 2001. The mesospheric quasi-2-day wave over Tirunelveli (8.7°N). *Journal of Atmospheric and Solar-Terrestrial Physics* 63, 975–985.
- Hagan, M.E., Forbes, J.M., Vial, F., 1993. Numerical investigation of the propagation of the quasi-2-day wave into the lower thermosphere. *Journal of Geophysical Research* 98, 23193–23205.
- Harris, T.J., Vincent, R.A., 1993. The quasi-2-day wave observed in the equatorial middle atmosphere. *Journal of Geophysical Research* 98, 10481–10490.
- Jacobi, C., 1998. On the solar cycle dependence of winds and planetary waves as seen from midlatitude D1 LF mesopause region wind measurements. *Annales Geophysicae* 16, 1534–1543.
- Jacobi, Ch., Schindler, R., Kürschner, D., 1997. The quasi two-day wave as seen from D1 LF wind measurements over Central Europe (52°N, 15°E) at Collm. *Journal of Atmospheric and Solar-Terrestrial Physics* 59, 1277–1286.
- Jacobi, C., Schindler, R., Kuerschner, D., 1998. Non-linear interaction of the quasi-2-day wave and long-term oscillations in the summer midlatitude mesosphere region as seen from LF D1 wind measurements over Central Europe (Collm, 52°N, 15°E). *Journal of Atmospheric and Solar-Terrestrial Physics* 60, 1175–1191.
- Kopecky, M., Kuklin, G., 1971. About 11-year variation of the mean life duration of a group sun spots. *Issledovanie Geomagnetizm i Aeronomi Fizika Solntsa* 2, 167.
- Lieberman, R.S., 1999. Eliassen–Palm fluxes of the 2-day wave. *Journal of the Atmospheric Sciences* 56, 2846–2861.
- Lieberman, R.S., 2002. Corrigendum to “Eliassen–Palm fluxes of the 2-day wave”. *Journal of the Atmospheric Sciences* 59, 2625–2627.
- Manson, A.H., Meek, C.E., Chshyolkova, T., Avery, S.K., Thorsen, D., MacDougall, J., Hocking, W., Murayama, Y., Igarashi, K., Namboothiri, S.P., Kishore, P., 2004. Longitudinal and latitudinal variations in dynamic characteristics of the MLT (70–95 km): a study involving CUJO network. *Annales Geophysicae* 22, 347–365.
- Meek, C.E., Manson, A.H., Franke, S.J., Singer, W., Hoffmann, P., Clark, R.R., Tsuda, T., Nakamura, T., Hagan, M., Fritts, D.C., Isler, J., Portnyagin, Yu., 1996. Global study of northern hemisphere quasi-2-day wave events in recent summers near 90 km altitude. *Journal of Atmospheric and Terrestrial Physics* 58, 1401–1411.
- Muller, H.G., 1972. Long-period meteor wind oscillations. *Philosophical Transactions of the Royal Society of London* 271, 585–598.
- Muller, H.G., Nelson, L., 1978. A travelling quasi-2-day wave in the meteor region. *Journal of Atmospheric and Terrestrial Physics* 40, 761–766.
- Norton, W.A., Thuburn, J., 1996. The two-day wave in a middle atmosphere GCM. *Geophysical Research Letters* 23, 2113–2116.
- Nozawa, S., Imaida, S., Brekke, A., Hall, C.M., Manson, A.H., Meek, C.E., Oyama, S., Dobashi, K., Fujii, R., 2003. The quasi 2-day wave observed in the polar mesosphere. *Journal of Geophysical Research* 108 (D2), 4039.
- Palo, S.E., Avery, S.K., 1995. Observations of the meridional quasi-two-day wave in the mesosphere and lower thermosphere at Christmas Island. *The Upper Mesosphere and Lower Thermosphere: A Review of Experiment and Theory*, Geophysical Monograph Series, No. 87, American Geophysical Union, pp. 101–110.
- Pancheva, D., 2000. Evidence for non-linear coupling of planetary waves and tides in the lower thermosphere over Bulgaria. *Journal of Atmospheric and Solar-Terrestrial Physics* 62, 115–132.
- Pancheva, D., Mukhtarov, P., 2000. Wavelet analysis on transient behaviour of tidal amplitude fluctuations observed by meteor radar in the lower thermosphere over Bulgaria. *Annales Geophysicae* 18, 316–331.
- Pancheva, D., Beard, A.G., Mitchell, N.J., Muller, H., 2000. Non-linear interactions between planetary waves in the mesosphere/lower thermosphere region. *Journal of Geophysical Research* 105, 157–170.
- Pancheva, D., Mitchell, N.J., Hagan, M.E., Manson, A.H., Meek, C.E., Luo, Y., Jacobi, Ch., Kuerschner, D., Clark, R.R., Hocking, W.K., MacDougall, J., Jones, G.O.L., Vincent, R.A., Reid, I.M., Singer, W., Igarashi, K., Fraser, G.I., Nakamura, T., Tsuda, T., Portnyagin, Yu., Merzlyakov, E., Fahrutdinova, A.N., Stepanov, A.M., Poole, L.M.G., Malinga, S.B., Kashcheyev, B.L., Oleynikov, A.N., Riggan, D.M., 2002a. Global-scale tidal structure in the mesosphere and lower thermosphere during the PSMOS campaign of June–August 1999 and comparisons with the global-scale wave model. *Journal of Atmospheric and Solar-Terrestrial Physics* 64, 1011–1035.
- Pancheva, D., Merzlyakov, E., Mitchell, N.J., Portnyagin, Yu., Manson, A.H., Jacobi, Ch., Meek, C.E., Luo, Y., Clark, R.R., Hocking, W.K., MacDougall, J., Muller, H.G., Kuerschner, D., Jones, G.O.L., Vincent, R.A., Reid, I.M., Singer, W., Igarashi, K., Fraser, G.I., Fahrutdinova, A.N., Stepanov, A.M., Poole, L.N.G., Malinga, S.B., Kashcheyev, B.L., Oleynikov, A.N., 2002b. Global-scale tidal variability during the PSMOS campaign of June–August 1999: interaction with planetary waves. *Journal of Atmospheric and Solar-Terrestrial Physics* 64, 1865–1896.
- Pfister, L., 1985. Baroclinic instability of easterly jets with applications to the summer mesosphere. *Journal of the Atmospheric Sciences* 42, 313–330.
- Plumb, R.A., 1983. Baroclinic instability of the summer mesosphere: a mechanism for the quasi-two-day wave? *Journal of the Atmospheric Sciences* 40, 262–270.
- Plumb, R.A., Vincent, R.A., Craig, R.L., 1987. The quasi-2-day wave event of January 1984 and its impact on the mean mesospheric circulation. *Journal of the Atmospheric Sciences* 44, 3030–3036.

- Raghava Reddi, C., Geetha, A., Lekshmi, K.R., 1988. Quasi-2-day wave in the middle atmosphere over Trivandrum. *Annales Geophysicae* 6, 231–238.
- Randel, W.J., 1994. Observations of the 2-day wave in NMC stratospheric analysis. *Journal of the Atmospheric Sciences* 51, 306–313.
- Riggin, D.M., Meyer, C.K., Fritts, D.C., Jarvis, M.J., Murayama, Y., Singer, W., Vincent, R.A., Murphy, D.J., 2003. MF radar observations of seasonal variability of semidiurnal motions in the mesosphere at high northern and southern latitudes. *Journal of Atmospheric and Solar-Terrestrial Physics* 65, 483–493.
- Rodgers, C.D., Prata, A.J., 1981. Evidence for a travelling 2-day wave in the middle atmosphere. *Journal of Geophysical Research* 86, 9661–9664.
- Salby, M.L., 1981a. Rossby normal modes in nonuniform background configurations I, simple fields. *Journal of the Atmospheric Sciences* 38, 1803–1826.
- Salby, M.L., 1981b. Rossby normal modes in nonuniform background configurations II, equinox and solstice conditions. *Journal of the Atmospheric Sciences* 38, 1827–1840.
- Salby, M.L., Callaghan, P.F., 2001. Seasonal amplification of the 2-day wave: relationship between normal mode and instability. *Journal of the Atmospheric Sciences* 58, 1858–1869.
- Salby, M.L., Roper, R., 1980. Long-period oscillations in the meteor region. *Journal of the Atmospheric Sciences* 37, 237–244.
- Thayaparan, T., Hocking, W.K., MacDougall, J., 1997a. Amplitude, phase and period variations of the quasi-2-day wave in the mesosphere and lower thermosphere over London, Canada (43°N, 81°W), during 1993 and 1994. *Journal of Geophysical Research* 102, 9461–9478.
- Thayaparan, T., Hocking, W.K., MacDougall, J., Manson, A.H., Meek, C.E., 1997b. Simultaneous observations of the 2-day wave at London (43°N, 81°W) and Saskatoon (52°N, 107°W) near 91 km altitude during the two years of 1993 and 1994. *Annales Geophysicae* 15, 1324–1339.
- Torrence, C., Compo, G., 1998. A practical guide to wavelet analysis. *Bulletin of the American Meteorological Society* 79, 61–78.
- Tsuda, T., Kato, S., Vincent, R.A., 1988. Long period oscillations observed by the Kyoto meteor radar and comparison of the quasi-2-day wave with Adelaide MF radar observations. *Journal of Atmospheric and Terrestrial Physics* 50, 225–230.
- Walterscheid, R., Vincent, R., 1996. Tidal generation of the phase-locked 2-day wave in the southern hemisphere summer by wave–wave interactions. *Journal of Geophysical Research* 101, 26567–26576.
- Ward, W.E., Yang, D.Y., Solheim, B.H., Shepherd, G.G., 1996. Observations of the 2-day wave in WINDII data during January 1993. *Geophysical Research Letters* 23, 2923–2926.
- Williams, C.R., Avery, S., 1992. Analysis of long-period waves using the mesosphere stratosphere–troposphere radar at Poker Flat, Alaska. *Journal of Geophysical Research* 97, 855–861.
- Wu, D.L., Hays, P.B., Skinner, W.R., Marshall, A.R., Burrage, M.D., Lieberman, R.S., Ortland, D.A., 1993. Observations of the quasi-2-day wave from the high resolution Doppler imager. *Geophysical Research Letters* 20, 2853–2856.